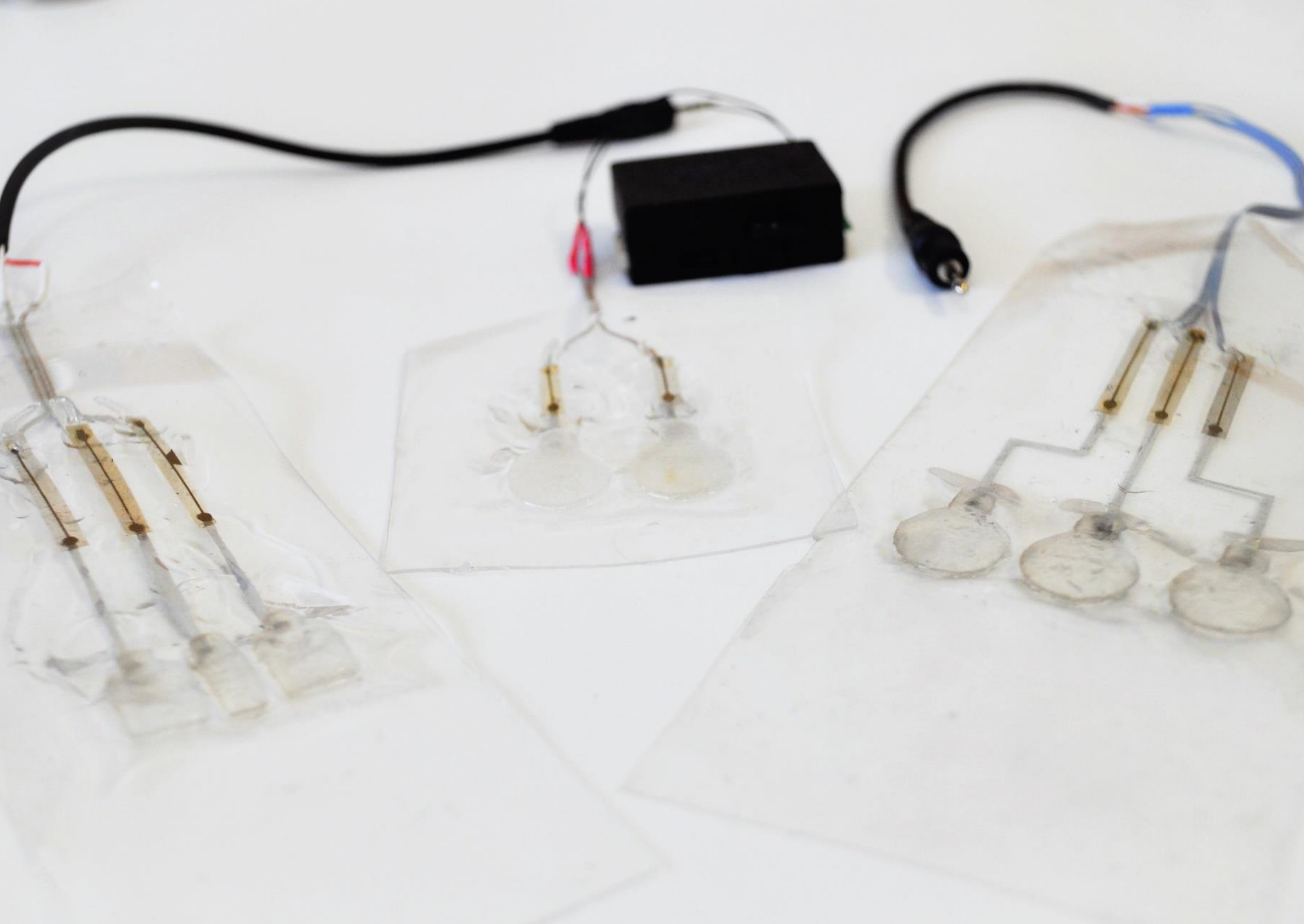

Tatiana Alexandra Fernandes Patrício

Hydrogel-PDMS conjunctions for Biomonitoring Patches

Thesis submitted to the University of Coimbra for compliance with the requirements for the degree of Master in Biomedical Engineering under the scientific supervision of PhD Mahmoud Tavakoli (UC) and PhD Jorge Coelho (UC).

September 2017

· U C ·

UNIVERSIDADE DE COIMBRA

FCTUC FACULDADE DE CIÊNCIAS
E TECNOLOGIA
UNIVERSIDADE DE COIMBRA

Tatiana Alexandra Fernandes Patrício

Hydrogel-PDMS conjunctions for Biomonitoring Patches

Thesis submitted to the University of Coimbra for the degree
of Master in Biomedical Engineering

Supervisors:

Prof. Dr. Mahmoud Tavakoli

Prof. Dr. Jorge Coelho

Coimbra, Setembro 2017

This work was supported by:

INSTITUTE OF SYSTEMS AND ROBOTICS
UNIVERSITY OF COIMBRA

Information and Communication Technologies Institute
Carnegie Mellon | PORTUGAL
AN INTERNATIONAL PARTNERSHIP

SML INTEGRATED SOFT MATERIALS LABORATORY
for human-compatible machines and electronics

POLYSYC
POLYMER SYNTHESIS AND CHARACTERIZATION

FCT
Fundação para a Ciência e a Tecnologia
MINISTÉRIO DA CIÊNCIA, TECNOLOGIA E ENSINO SUPERIOR

Esta cópia da tese é fornecida na condição de que quem a consulta reconhece que os direitos de autor são pertença do autor da tese e que nenhuma citação ou informação obtida a partir dela pode ser publicada sem a referência apropriada.

This copy of the thesis is supplied on condition that anyone who consults it understands to recognize that its copyright rests with its author and that no quotation from the thesis and no information derived from it may be published without proper acknowledgement.

“The way to get started is to quit talking and begin doing.”

Walt Disney

Agradecimentos

Ao longo destes 5 anos em Coimbra, para além de ter vivenciado mil e muitas aventuras que esta cidade maravilhosa me proporcionou, tive a oportunidade de conhecer pessoas incríveis. Por isso, agradeço a Coimbra pelo conhecimento, histórias e pessoas que levo para a vida.

Aos meus pais, que me fizeram aquilo que sou hoje. Obrigada por me terem providenciado esta oportunidade e pelo apoio incondicional. À minha família toda em geral, um grande obrigada.

A ti Rui pelo carinho, apoio, paciência e pela força. Obrigada por teres partilhado estes anos comigo, com todas as aventuras e desafios que espero poder continuar a partilhar.

A todos os meus amigos, desde colegas de curso e ao Zoo que me acompanharam nestes anos em Coimbra. Aos meus amigos de sempre, que me acompanharam da Madeira para cá ou que sempre fizeram questão de estar presentes, apesar da distância, o meu enorme obrigado. Dizem que amizades que duram mais 7 anos provavelmente durarão para toda a vida. É isso que espero e acredito.

Aos meus colegas de laboratório no DEEQ, Inês, Maria Inês e Rafael, obrigada pela boa disposição e motivação nos dias mais difíceis. Especialmente obrigada pela ajuda que me deram muitas vezes para o sucesso do procedimento experimental.

Agradeço aos meus orientadores Jorge Coelho e Mahmoud Tavakoli pela gratificante oportunidade que me ofereceram de conhecer um pouco melhor a área interessante em que se insere esta tese. Agradeço a ambos por me terem também disponibilizado acesso aos

laboratórios e a todos os materiais e instrumentos necessários para concluir com sucesso este projeto. Em particular ao Professor Mahmoud pelos sábio conselhos. Agradeço também à Joana Góis pela paciência, pelos conselhos e pela ajuda ao longo deste trabalho. Ao Professor Pedro Faia, agradeço a disponibilidade e a indispensável ajuda que nos prestou na realização dos testes de impedância.

Para terminar, não poderei esquecer os colegas de laboratório do ISR pela incrível ajuda que me prestaram, especialmente o João, o Pedro, o Rui Rocha e o Daniel, com quem tive um enorme gosto de trabalhar. Foram incansáveis desde ao primeiro ao último dia.

Abstract

Wearable health device that allows the continuous monitoring of physiological signals could be a powerful tool for early diagnosis, monitoring chronic diseases and therapeutics. Thus, wearable health devices have gained a lot of attention from the scientific community and from companies related to this area.

Over the last few years, wearable sensors for biomonitoring have been developed. However, most of them do not have enough stretchability to follow the curvature and movement of the body. Tough hydrogels are an attractive material since they are mostly composed of water, are permeable to different molecules and exhibit good stretchability. Their biophysical similarity with biological tissues makes them an interesting material to use as skin interface. The combination of these tough hydrogel with PDMS can increase their mechanical robustness and the range of possible applications.

In this dissertation, the fabrication process of hydrogel-PDMS hybrid is combined with the fabrication process of stretchable multilayer systems. Based on this successful combination, two different possible application of biomonitoring patches with hydrogel-PDMS electrodes were demonstrated: GSR and EMG sensors.

Through an impedance analysis, we demonstrated that hydrogel-PDMS electrodes have low electrode-skin impedance, leading to a good quality of the biological signal. This was proven by the good signal obtained with the EMG sensors.

Moreover, GSR patch was used to measure skin resistance changes during exercise and sonorous stimuli. The changes were clear on the physical exercise test, however, on the stress test, some of the stimuli did not cause notable changes in the skin resistance. The more evident emotion was fear induced by a horror movie, which caused a visible decrease in skin resistance.

In summary, this dissertation should be a useful guideline for hydrogel-PDMS electronics fabrications, mainly for future application on wearable health devices.

Keywords: Wearable heath devices; Tough hydrogels; PDMS; Hydrogel-PDMS electrodes; Biomonitoring; Stretchable electronics.

Resumo

Os dispositivos de saúde vestíveis, que permitem fazer uma monitorização contínua dos sinais fisiológicos, podem ser uma ferramenta poderosa para realizar diagnósticos precoces, monitorizar doenças crónicas e executar regimes terapêuticos. Por estas razões, os dispositivos de saúde vestíveis têm atraído uma vasta atenção da comunidade científica e de um grande número de empresas relacionadas com esta área.

Ao longo dos últimos anos, têm-se desenvolvido sensores vestíveis para biomonitorização. Contudo, uma grande parte destes dispositivos não possui deformabilidade suficiente para se adaptar à curvatura e ao movimento do corpo. Neste contexto, os hidrogéis robustos são um material atrativo uma vez que são maioritariamente compostos por água, possuem permeabilidade para diferentes moléculas e apresentam boa deformabilidade. A sua semelhança biofisiológica com os tecidos biológicos faz deles um material interessante para utilização em interface com a pele. A combinação destes hidrogéis robustos com PDMS pode aumentar a sua robustez mecânica e o leque de possíveis aplicações.

Nesta dissertação, o processo de fabricação do híbrido hidrogel-PDMS é combinado com o processo de fabricação de sistemas de multicamadas deformáveis. Baseadas no sucesso desta combinação, foram demonstradas duas possíveis aplicações diferentes para os adesivos de biomonitorização com elétrodos hidrogel-PDMS: sensores de GSR e sensores de EMG.

Através de uma análise de impedância, demonstramos que os elétrodos hidrogel-PDMS possuem baixa impedância elétrodo-pele, o que permite obter um sinal biológico de boa qualidade. Isto foi provado pelo bom sinal obtido com os sensores de EMG. Além disto, o adesivo de medição da GSR foi utilizado para medir alterações na resistência da pele, durante a realização de exercício físico e exposição a estímulos sonoros. O teste de exercício físico produziu alterações evidentes mas alguns dos estímulos utilizados no teste de stresse não provocaram alterações percetíveis na resistência da pele. A emoção mais evidente foi o medo induzido pela visualização de um excerto de um filme de terror, que causou uma visível diminuição na resistência da pele.

Em suma, pretende-se que esta dissertação seja um guia útil para a fabricação de dispositivos eletrónicos híbridos de hidrogel-PDMS, sobretudo para futuras aplicações em dispositivos de saúde vestíveis.

Palavras-chave: Dispositivos de saúde vestíveis; Hidrogéis Robustos; PDMS; Elétrodos de Hidrogel-PDMS; Biomonitorização; Eletrónica deformável.

Contents

Agradecimentos **x**

Abstract **xi**

Resumo **xiii**

Acronyms **xvii**

List of Figures **xix**

List of Tables **xxiii**

1 Introduction **1**

1.1 Motivation and Goals 6

2 State of the art **7**

2.1 PDMS electronics 7

2.2 Hydrogel 11

2.3 Hydrogel-PDMS hybrids 14

3 Materials and methods **19**

3.1 Materials 19

3.1.1 Hydrogels and tough hydrogels 19

3.1.2 PDMS 21

3.1.3 Liquid Metal - EGaIn 23

3.1.4 Flexible PCB 24

3.2 Fabrication Methods 25
3.2.1 Fabrication of hydrogel-PDMS hybrid 25
3.2.2 Fabrication of a soft EMG sensor 29
3.2.3 Fabrication of GSR sensor 32
3.3 Experimental tests 33
3.3.1 Dehydration test 33
3.3.2 Impedance Analysis 33
3.3.3 Soft EMG - signal acquisition 36
3.3.4 GSR measurement 37

4 Results **39**
4.1 Tough Hydrogel-PDMS hybrid 39
4.2 Dehydration test 40
4.3 Impedance analysis 41
4.4 Soft EMG sensor and signal acquisition 44
4.5 GSR sensor and measurements 50
4.6 Conclusion 53

5 Conclusions **55**
5.1 Future work 56

Appendices **67**

Acronyms

AgNW Silver Nanowires

BP Benzophenone

CNT Carbon Nanotube

cPDMS Carbon Polydimethylsiloxane

ECG Electrocardiogram

EEG Electroencephalogram

EGaIn Eutectic Gallium-Indium

EMG Electromyogram

FPCB Flexible Printed Circuit Board

GSR Galvanic Skin Response

ITO Indium Tin Oxide

MBAA N, N'-methylenebisacrylamide

MEMS Micro Electro Mechanical Systems

PAAm Polyacrylamide

PDMS Polydimethylsiloxane

SWCNT	Single-Walled Carbon Nanotube
UV	Ultraviolet
VIA	Vertical Interconnect Access
zPDMS	z-axis Polydimethylsiloxane (conductive composite)

List of Figures

1.1 Forecast of the market distribution of wearable sensor types in 2020. . . . 1

1.2 A multichannel EMG sensor that attaches to the skin and can cover a large area. 2

1.3 A rugged stretchable electronic systems for monitoring of different physiological signals. 3

1.4 Sweat analysis systems. 4

2.1 Fracture energy of some materials and respective work to rupture. Includes also the length of flaw sensitivity. Values of natural rubbers are similar to the skin. 7

2.2 iSkin consist on a pattern layer of cPDMS on a PDMS layer. 9

2.3 10

2.4 A transparent and stretchable hydrogel electronic device where LED lights connected by stretchable titanium wires were embedded on the matrix. . . 11

2.5 Performance of some stretchable conductors. 13

2.6 Examples of applications with conductive hydrogels. 14

2.7 Bonding of tough hydrogels to the solid substrate. 16

2.8 Conductive hydrogel circuit pattern on a elastomer. When connected to a AC power source it could light up a LED, even under deformation. 16

2.9 Hydrogel-PDMS living patch. 17

3.1 Polymer networks of three types of hydrogels. 20

3.2 Chemical structure of PDMS. 21

3.3 Liquid metal alloys enable the fabrications of stretchable circuits. 23

3.4 The hybrid structure. 25

3.5 Surface modification of cured PDMS surface. (I) A benzophenone solution is applied over all surface. (II) After 2 minutes, the surface is washed with methanol and (III) dried with nitrogen gas. 26

3.6 Hydrogel preparation. (I) After degassed the pre-gel solution, (II) the solution is pulled to one syringe. (III) In another syringe, calcium sulfate and irgacure 2959 are introduced and thereafter, (IV) some drops of water bubbled with nitrogen gas are added on the tip of this syringe. (V) The two syringes are connected and the solutions are mixed. 27

3.7 (A) The mould used to developed the hydrogel-PDMS hybrid. With the help of silicone grease, the rubber frame is sealed on top of a glass slide. The inner rectangular on the rubber frame has 70x70x1 (length x width x thickness). (B) The assembling of the hydrogel and treated PDMS on the mold. 28

3.8 Resume schematic of the fabrication process of hydrogel-PDMS hybrid. . 28

3.9 The design used to create the soft and stretchable EMG sensor onto PDMS layers. 29

3.10 **Hydrogel-PDMS electrodes.** **(A)** The hydrogel-PDMS hybrid is cut to the required shape using a laser cutting system. **(B)** After introducing conductivity, the thickness of the electrodes slightly increases. They have 15 mm of diameter. 30

3.11 Schematics and respective photos of the fabrication method of the soft EMG. 32

3.12 **Dehydration test:** **(A)** sample left in air ambient and **(B), (C)** sample used over the skin. 33

3.13 Equivalent circuit model of electrode-skin impedance. 34

3.14 Electrodes used in the impedance measure test: **(A)** Ag/AgCl electrodes, **(B)** Hydrogel-PDMS electrodes, **(C)** zPDMS electrodes, **(D)** Stainless steel electrodes,**(E)** Tattoo electrodes and **(F)** cPDMS electrodes. 35

3.15 **(A)** The precision impedance analyser used. **(B)** Hydrogel-PDMS electrodes placed on the subject ventral side of the right forearm. 36

3.16 The soft EMGs developed were used to detect the **(B)** flexor carpi radialis muscle and the **(C)** flexor carpi ulnaris muscles. 36

3.17 The GSR system was placed on the upper-arm of the subject and fixed with an armband. 37

4.1 **(A)** Hydrogel-PDMS hybrid. **(B)** This hybrid is tough and can sustain high deformation. 39

4.2 Weight ratio loss over dehydration time for both samples. 40

4.3 Photos of the hydrogel–elastomer hybrid sample in contact with the skin during the dehydration time. 41

4.4 Experimental results (blue) and the fitting curve (red) for each electrode-skin impedance frequency response and the respective mean square error associated to the fitting curve. 41

4.5 Experimental results (blue) and the fitting curve (red) for both hydrogel-PDMS electrode-skin impedance frequency response. 44

4.6 **(A)** Two soft EMG sensors were developed with hydrogel-PDMS electrodes. **(B)** Square hydrogel-electrodes were used to fabricate one of the EMG sensors and **(C), (D)** round electrodes for the other. 45

4.7 **(A)** Movement of opening the hand. **(B)** Signal with the stainless steel electrodes. **(C)** Signal with the round hydrogel-PDMS electrodes. 46

4.8 **(A)** Movement of fist clenching. **(B)** Signal with the stainless steel electrodes. **(C)** Signal with the hydrogel-PDMS electrodes. 47

4.9 **(A)** Flexion of the wrist. **(B)** Signal with the stainless steel electrodes. **(C)** Signal with the hydrogel-PDMS electrodes. 48

4.10 Signals acquired with the **(A), (B)** opening of the hand, **(C),(D)** clenching the wrist and **(C),(D)** during wrist flexion. 49

4.11 GSR sensor proposed in this work. The sensor consists in a multilayer system with hydrogel-PDMS electrodes, EGaIn and FPCBs as interconnects. 50
4.12 Skin resistance measures over time during daily activities for **(A)** Stainless steel electrodes and **(B)** the hydrogel-PDMS electrodes. 51
4.13 Skin resistance signal collected during physical exercise (blue) and the filtered signal (red). 51
4.14 **(A)** Detected changes on skin resistance induced by sonorous stimuli (blue) and the filtered signal (red). **(B)** Zoom from area of interested. . . . 52

List of Tables

3.1 Composition of the tough hydrogel with 85 wt.% of water. 26

4.1 Circuit components values for all electrodes with approximately the same area and distance between them. 42

4.2 Circuit components values for the two types of hydrogel-PDMS electrodes per square centimetre. 44

Chapter 1

Introduction

The increase in demand for biomonitoring is the main motivation for the development of wearable devices market, that is predicted to reach over $150 billion by 2027 [1]. The trend of home healthcare, developments in wireless data transmission, alerting mechanisms and real-time control, along with the need for comfortable and non-invasive alternatives for monitoring are some of the growth opportunities for the wearable medical devices market.

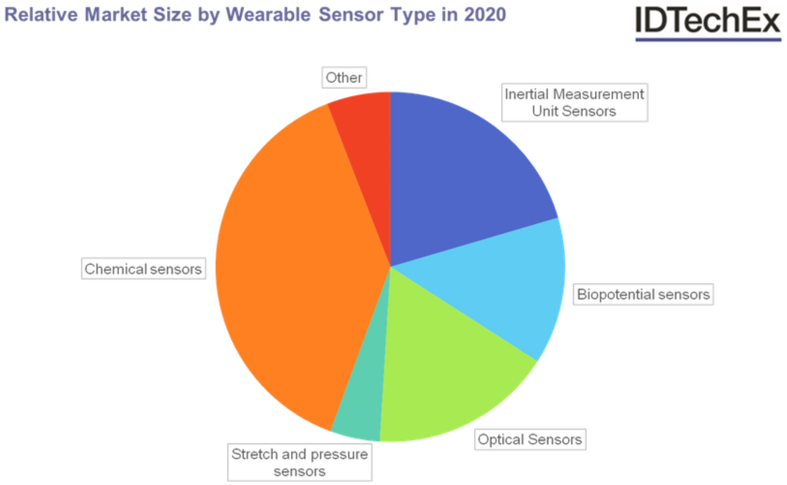

Figure 1.1: Forecast of the market distribution of wearable sensor types in 2020 [2].

Wearable health devices allow different types of interventions in the field of medical and personal care, through monitoring of chemical and physical body properties using sensors. In addition, remote healthcare monitoring minimizes the healthcare expenses in hospitals or nursing homes. Sensors are a diverse component in wearable devices. In the plot from figure 1.1, it is possible to observe the distribution of wearable sensor types in 2020 [2]. It is estimated that by 2025 there will be 3 billion of wearable sensors and over 30% of them will be new types of sensors [2]. However, most of today's wearable health devices are rigid, since they are made of large and stiff components making it uncomfortable to wear. Therefore, developments in the field of stretchable electronics are the best way known to achieve a skin-like biomonitoring patch.

A stretchable biomonitoring patch that follows the shape of the human body can be used to record real-time information, continuous monitoring of the human health and motion activities. There are a diversity of physiological signals that can be measured such as the electrical activities of the brain through an electroencephalogram (EEG) [3, 4], heart with an electrocardiogram (ECG) [4, 5] and muscles with an electromyogram (EMG) [4, 6, 7]. Moreover, blood pressure, blood oxygenation [8], heart rate [8], body temperature [9] and skin conductance through galvanic skin response (GSR) [10–12] can also be quantified. Each of these signals has important clinical informations about body function. Monitoring these physiological signals can be helpful for diagnosis, treatments, monitoring chronic diseases, rehabilitation and for human-machine interfaced devices (HMIs) [13, 14]. Therefore, interest in employing stretchable electronics in biomonitoring has increased.

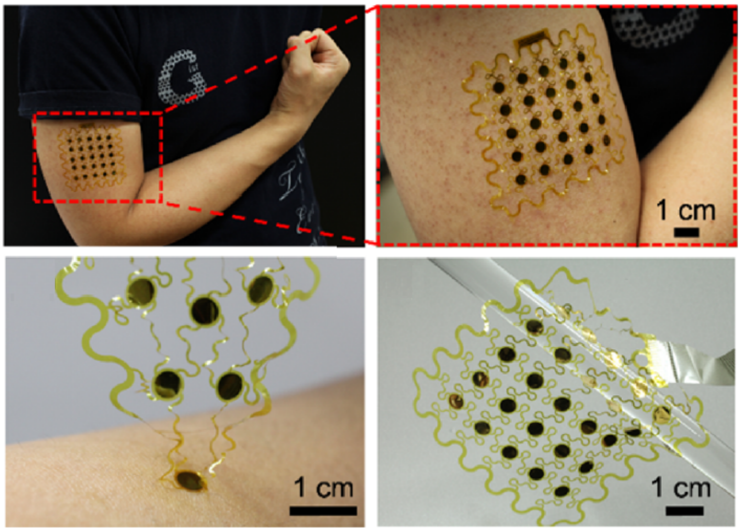

Figure 1.2: A multichannel EMG sensor that attaches to the skin and can cover a large area (adapted from [7]).

Monitoring muscle activity can be an important tool for self-rehabilitation, diagnosis of neuromuscular diseases and observe muscular movements for medical treatments [7]. EMG signal can be used as input for games or to control prosthesis [13]. An armband composed of EMG sensors was recently commercialized [15], it reads the electrical activity of muscles to control multimedia devices, robots, or to play music hands-free. Due to this variety of applications, there is a great interesting in developing a stretchable and comfortable systems for signal acquisition.

Recently, a reusable multichannel EMG was demonstrated with gold and titanium electrodes that allows detecting of different muscles on its contact area [7]. Moreover, monitoring of some physiological signals such as hydration state, electrical activity (ECG, EMG, EEG) and blood oxygenation were achieved with a combination of optical, electrical and radio-frequency sensors [16]. Bi-layers of gold (Au) and chromium (Cr) serpentine electrodes were bond to PMDS and polyimide substrates. A combinations of silicone materials with elastic fabrics such as nylon was study in order to achieved a rugged platform for the system (figure 1.3). However, both of these electrodes are not very stretchable and given the fabrication process are not suitable for scalable production.

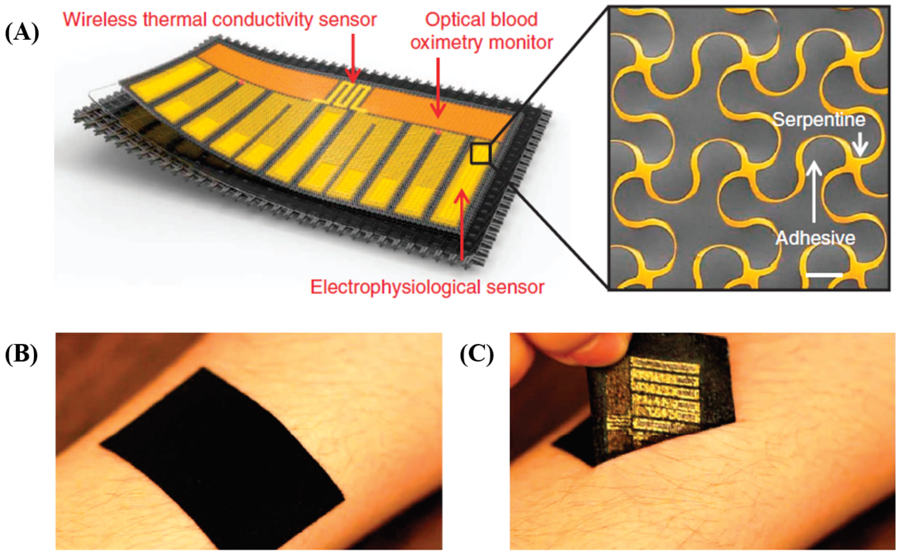
(A)
Wireless thermal conductivity sensor
Optical blood oximetry monitor
Serpentine
Adhesive
Electrophysiological sensor
(B)
(C)

Figure 1.3: A rugged stretchable electronic systems for monitoring of different physiological signals. **(A)** Illustration of the several layers which includes the active electronics, elastomer coating and a stretchable fabric. **(B)** The applications of the device on the skin and **(C)** the detachment. (adapted from [16]).

Besides the previously described physiological signals, sweat is a body fluid that can be used for health monitorization. This complex mixture incorporates different electrolytes such as chloride, sodium and potassium along with molecules like lactate and glucose [17]. The composition of sweat can change according to human health conditions. Therefore, sweat can be used for biomonitoring of dehydration, and diseases like cystic fibrosis and childhood pancreatic disease [17]. Examples of achievements on sensors for sweat analysis includes a soft epidermal microfluidic device that is able to capture, storage and sensing of markers on sweat [18], or a thin microfluidic networks for time sequential capture of sweat samples [17].

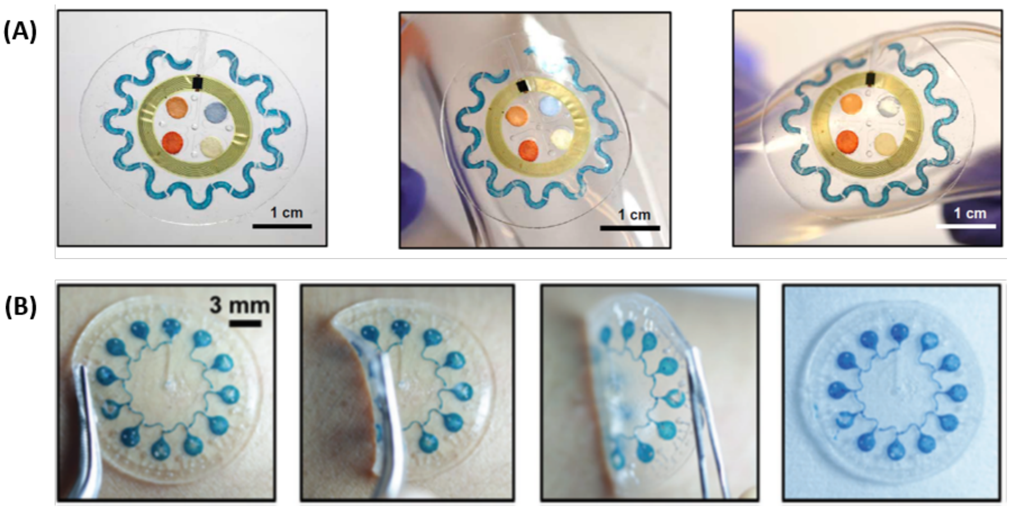

Figure 1.4: Sweat analysis systems. **(A)** Microfluidic systems for sweat capture and colorimetric sensing [18]. **(B)** Epidermal microfluidic device for sweat chrono-sampling with dyed water attached to the skin [17].

When exposed to stressful situations the sweat secretion from exocrine glands increase due to sympathetic nervous system response. Consequently, as sweat is an electrolyte and good conductor, this increased secretion would result in an increase of the skin conductance [11]. These variations on the conductance of the skin are known as galvanic skin response (GSR) or electro-dermal activity (EDA) and reflect the activity of the sympathetic nervous system in stress or emotional situations [11]. Therefore, continuous non-invasive monitoring of GSR enables the observation of sympathetic nervous systems activity and can give important information that limited time monitoring does not allow. Besides, it is important to do measurements in a home environment since hospitals or laboratories can have psycho-physiological conditions on the person [11]. A wearable sensor was demonstrated for GSR measurements from the back of an user [12]. The electrodes were embedded on a thin flexible printed circuit board covered by a silicon layer. As sensing electrodes, a conductive foam was used plated with a conductive material (Ni/Cu) that provides electrical conductivity to measure the skin conductance response to and auditory stimuli. However, there is lack of stretchable devices for GSR measurements.

Sweat analysis can be used to monitoring several health indices through identifying changes in its composition. After collection, the sweat may be analysed with biomarkers, chemical reactions, conductivity measurements, etc. Regardless of the type of posterior or continuous analysis performed, a biomonitoring patch capable of sweat analysis is, in fact, a Lab-On-A chip with materials that allow sweat collection. One of these materials that received an increasing attention during this previous years are hydrogels.

Hydrogels are mostly composed of water. They largely match properties of the human organ such as stretchability and adhere very easily to the skin. They can even be turned conductive with electrolyte solutions. All these properties make them a very attractive material for bio-monitoring patches, not only for sweat analysis but also for detection of electrical events of the body, e.g., EMG/ECG/EEG/GSR. Nevertheless, their mechanical properties are usually weak. This is a motivation for a hot topic of research: tough hydrogels. Such problem is solved, hydrogels become immediately the most attractive electrode for bio-monitoring.

1.1 Motivation and Goals

Materials and fabrication methods of stretchable electronics have experienced rapid advances during the last decade. It is in fact possible to fabricate multilayer stretchable circuits that can be mounted over the skin. Most of the previous works in this area used PDMS as the main substrate. PDMS is a stretchable, biocompatible, transparent and relatively low-cost material. Despite its advantages, it is not permeable to body liquids and contain no water on its constitution.

On the other hand, hydrogels exhibits some unique features such as high water capacity, permeability to various chemical and biological molecules including body fluids, biocompatibility and biodegradability [19]. Yet, their low robustness is a disadvantage. Due to the biophysical similarity between hydrogels and soft biological tissues, they show a great potential for biomedical applications, such as a skin interface for sensors. Hybrid combinations of hydrogels and PDMS have a higher potential since they complement each other enabling new applications. Until recently, most of existing hydrogel-elastomers hybrids had weak interfacial bonding, low robustness and difficulties in patterning microstructures [19]. In a recent publication in *Nature*, Yuk *et al* (2016) [19] reported a new method where these limitations are overcomed.

The main objective of this work is to obtain the know-how of the fabrication process of hydrogel-PDMS conjunctions based on the work of Yuk *et al* [19] and combine it with known fabrication process of PDMS-based stretchable electronics for developing biomonitoring patches. If successful, state of the art materials and fabrication methods used in stretchable electronics will be combine with the state of the art of conductive hydrogels as measuring electrodes. As a case study, we demonstrate an EMG sensor in which an hydrogel-PDMS hybrid is used as electrodes. Moreover, preliminary steps were done on a GSR sensor as another case study.

Chapter 2

State of the art

In the following chapter, recent state of the art on stretchable electronics is addressed. It includes PDMS electronics, hydrogels based stretchable electronics as well as hybrid combination of these two materials.

2.1 PDMS electronics

Soft materials exhibit a great potential on stretchable electronics applications including electronic skins, wearable devices and deformable electronics.

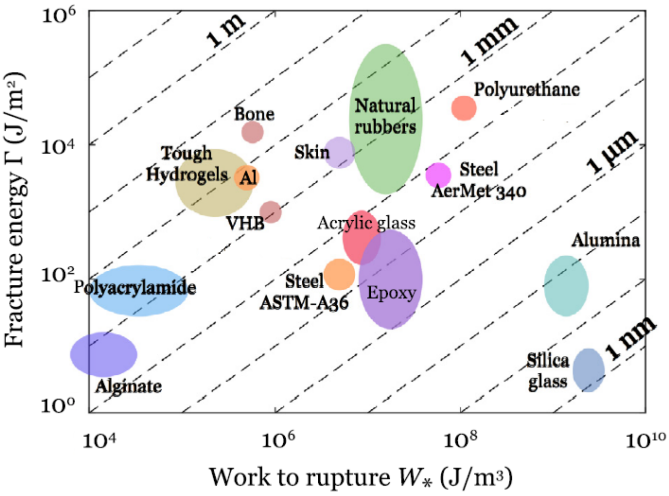

Figure 2.1: Fracture energy of some materials and respective work to rupture. Includes also the length of flaw sensitivity. Values of natural rubbers are similar to the skin [20].

Even though the search for stretchable materials continues to be thorough, there are already some materials, as PDMS, that exhibit high stretchability closer to the human skin. Rubbery materials, including PDMS have similar material properties to the skin, as can be seen in the plot from figure 2.1.

The use of soft elastomers as a carrier medium for electronic conductors give to stretchable electronics the ability to blend, twist and stretch. Stretchable conductors are important to achieve electronics with high stretchability while maintaining conductivity. Currently, most of stretchable conductors used include carbon grease [21], graphene [22], microcracked gold films [7], serpentine-shaped metallic wires [4], carbon nanotubes (CNTs) [23, 24], silver nanowires (AgNWs) [25, 26], copper nanowires (CuNWs) [27], liquid metal [28] and conductive polymers [6,29]. These conductive materials can be present in the form of thin film, fibres and combined with elastomers to form a composite.

In order to complete the desirable properties, such as large mechanical deformability, reliability, good adhesion, low cost and high yield, most of stretchable components use PDMS as a support matrix for embed stretchable conductors.

Recently, a stretchable skin-worn sensor named by iSkin was developed combining layers of PDMS and carbon doped PDMS (cPDMS). The iSkin is worn directly on the skin, it is a customizable thin, soft, flexible and stretchable (can be stretched up to 30%) [14]. Compared to others stretchable conductors, cPDMS may be more appealing due to its low cost and easy manufacturing. However, sometimes there are changes in the conductance and it may require a high concentration of carbon black particles [29]. Moreover, it is opaque which is important in some applications.

There is various example of combinations of stretchable conductors with PDMS, having all different mechanical and electrical properties. A non-transparent capacitive strain sensor based on AgNW-PDMS with 50% stretchability and a high conductivity (sheet resistance of 0.24 Ω/sq) was reported. The silver nanowires were embedded in an uncured PDMS layer forming a stretchable layer [25]. Others AgNW-PDMS composites were developed over the past few years. Park *et al* [30] designed a AgNW percolation micro-grids in a PDMS substrate. The final device had a low sheet resistance of 26.1 Ω/sq, high optical transmittance (85.8%) and a tensile strain of 30%. Moreover, a conductive AgNW-PDMS composite was made by spray-deposition of AgNW on a polydopamine-modified PDMS surface. A polydopamine layer was used as a way to enhance the bond with AgNW and PDMS by creating a highly hydrophilic surface on PDMS. These composite showed 80% of transmittance and low sheet resistance (35 Ω/sq). However, a lower stretchability than the previous ones (20%) was observed [26]. Besides silver nanowires, it is proven that carbon nanotubes (CNTs) also have good conductivity. Aligned CNT ribbons were embedded in PDMS to form a stretchable conductor that can sustain conductivity under repetitive strain cycles [23].

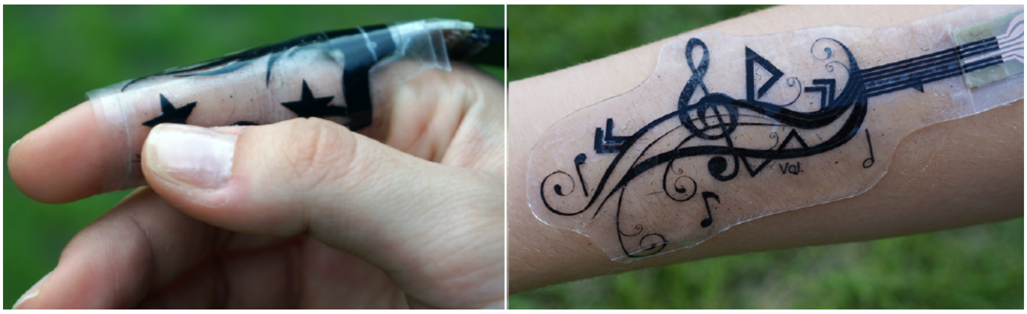

Figure 2.2: iSkin consist on a pattern layer of cPDMS on a PDMS layer [14].

A wearable and stretchable carbon nanotube strain sensor was reported for human-motion detection [24]. Thin films of single-walled carbon nanotubes (SWCNT) for strain sensor were aligned perpendicular to the strain axis on top of a PDMS substrate. In order to demonstrated the applications of these SWCNT films, a wearable device was made by combining the SWCNT films with electrodes (Ti/Au/Ti) and assembling them on clothes and bandage with PDMS glue. The bandage and SWCNT film device was fixed on the chest, throat in order to monitored respiration and speech respectively. Moreover, the SWCNT film device was used to detect and distinguish movements on the knee.

Although some of PDMS composites exhibit high stretchability and conductivity, the fabrication method of some thin polymer coating requires relatively expensive photolithography and metal evaporation in vacuum. Others nanomaterials fabrication process need high temperature, reducing atmosphere and it is a time-consuming process, which makes them not suitable for large scale applications. Even so, some processes are difficult to control, leading to nanomaterials with different shapes and sizes which may influence their properties.

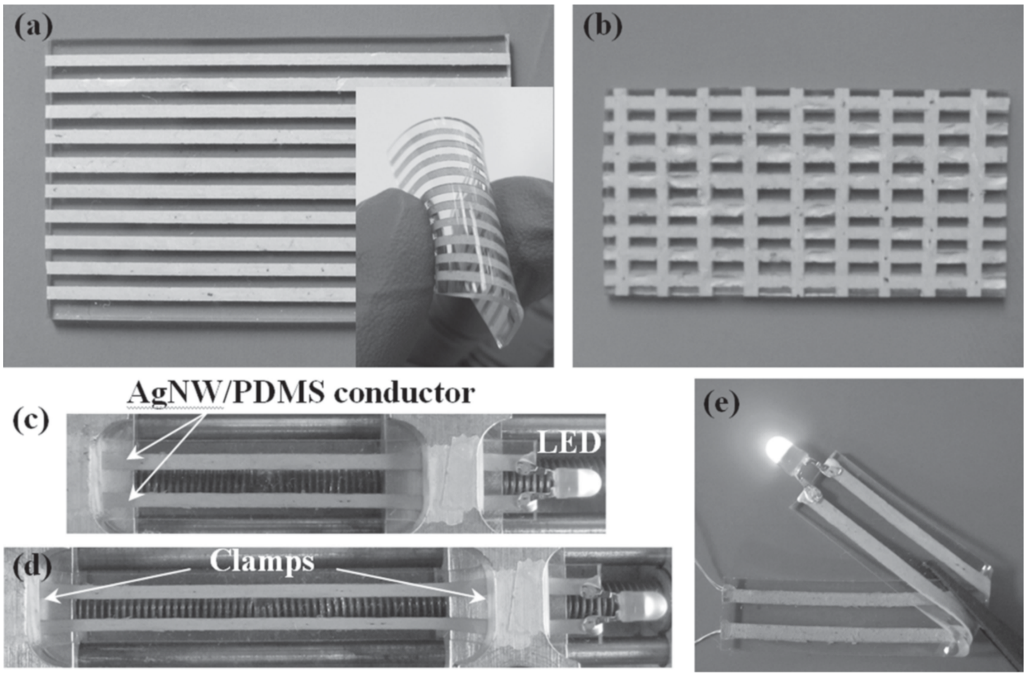

Figure 2.3: Stretchable AgNW-PDMS composite in a **(a)** parallel and **(b)** crossed patterned. **(c, d, e)** A led was lighted up with two AgNW-PDMS conductors. It sustained 50% strain and could be folded and the led would continue to work [25].

While many of these stretchable conductors can be used as interconnects in stretchable printed circuit boards (PCBs) and biomonitoring patches, they are not the best option as measuring electrodes. An ideal electrode for biomonitoring patches should match mechanical properties of the skin. Containing water, sticking to the skin and being permeable to biologic fluids and chemical molecules, such as chemical elements present in sweat, are some of the factors that can be seen in conductive hydrogels only, and none of the above cited materials can afford such properties.

2.2 Hydrogel

Since hydrogels are transparent, biocompatible soft materials that conform to tissues and can be stretched, they show a great potential for stretchable electronic devices. Additionally, they have high water content and can incorporate electrolytes which make them ionic conductive. Besides stretchable electronics, there are other fields where hydrogels can be applied to such as tissue engineering, cell culture systems, drug delivery systems, microfluidics, optics and soft robotics [31, 32]. However, their low mechanical strength can restrict their application [19]. Strategies to exceed this limitation have already been presented, such as tough hydrogels and also by combinations of hydrogels with mechanical robust materials [19, 33].

Due to their attractive applications in such different areas but mainly in electronics, cell culture systems and microfluidics, research on hydrogels received a boost in the recent years. Two main areas of research in hydrogels are relevant to this dissertation. First, researches on tough hydrogels and other solutions, in order to overcome the problems on the low mechanical strength. Second, researches on conductive hydrogels which allow ionic conductivity and signal transmission, such as ionic cable [34].

Hydrogel based stretchable devices have been recently studied, where it can be used as support matrix to embed rigid components [35] or as an ionic conductor [36]. Conductive hydrogels have been used in sensors and electrical signal transmission [33, 34, 37].

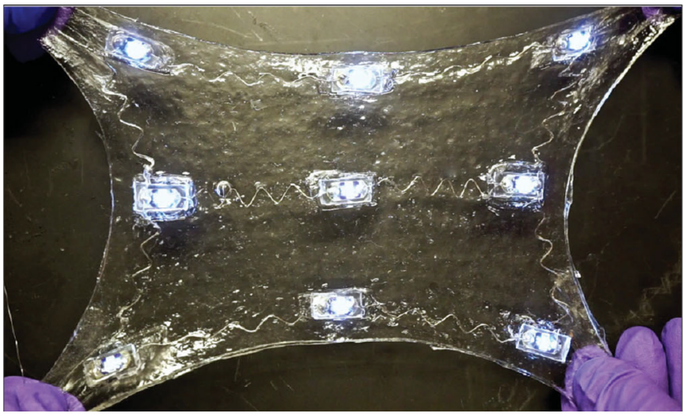

Figure 2.4: A transparent and stretchable hydrogel electronic device where LED lights connected by stretchable titanium wires were embedded on the matrix [35].

Multiple tough hydrogel-solid hybrids were reported with interfacial toughness over 1000 Jm^{-2}, where, through surface modification, they are bond chemically [33]. These included solid materials such as ceramics, glass, silicon, titanium and aluminium. The tough bonding was achieved by chemically anchoring the tough hydrogels to the non-porous surfaces through silanation of the surface, i.e, the surfaces are modify with a functional silane. The use of tough hydrogels allows an increase of interfacial toughness values from below 100 J m^{-2} up to 1500 J m^{-2}. Even when the hydrogel is at swollen state, the detaching behaviour from the surfaces is similar to the same hydrogel as prepare. In order to demonstrate the variety of applications that these tough hydrogel-solid hybrids allow a tough hydrogel superglues, hydrogel coatings for mechanical protection, hydrogel joints for robotic structures and even hydrogel-metal conductor were then developed [33]. Although the tough hydrogels exhibit high stretchability, most of these solid substrate used are not fully stretchable. Even so, this chemical anchoring shows the possibility of extremely tough bonding between hydrogels and solid surfaces and new applications for example for robust electronic devices.

The possibility of integrating ionic conductors on electronics and soft machines similar to the function of human body that transmits signals with ions have been proven in recent studies. For instance, Keplinger *et al* [36] described devices with ionic conductors that are highly stretchable, fully transparent and capable of operation at high frequencies and voltages. Their basic design consisted on placing a dielectric elastomer (VHB$^{\mathrm{TM}}$) between two membranes of polyacrylamide (PAAm) hydrogel containing NaCl salts, connected on each side with copper electrodes. This design was used to fabricate a large-strain actuator capable of fast voltage-induced deformation and a transparent loudspeaker that produces sound across the entire audible range [36]. A stretchable interconnect made by conductive hydrogel with the same principle, called ionic cable, was also demonstrated [34]. The ionic cable was used to transmit music signals by connecting it to a commercial electrical cable in both ends. Even when stretched to eight times its original length it still worked. It was also used as a interconnect to turn on light-emitting diode for more than 24 hours. Even with common hydrogels the ionic cable and the large-strain actuator showed a high stretchability, however replacing it with tough hydrogels could even enhance these properties.

Although conductive hydrogels exhibit higher resistivity than others electronic conductors, when high stretchability and transmittance are desire, they have shown lower sheet resistance that some electronics conductors (figure2.5) [36].

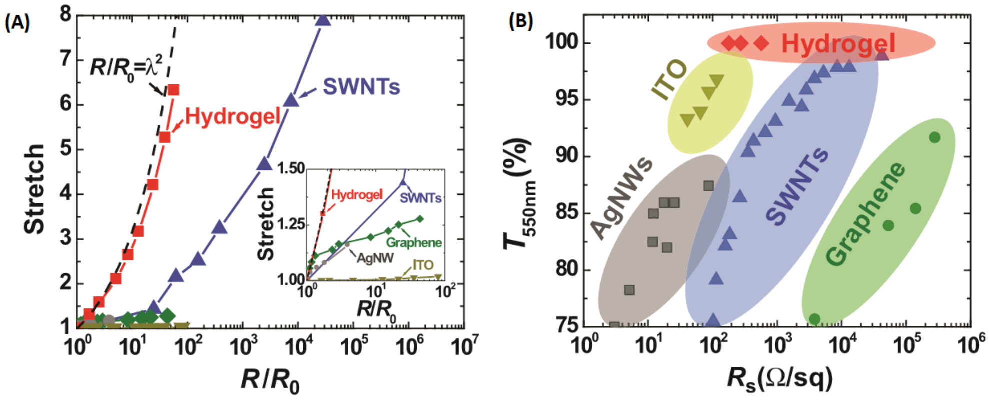

Figure 2.5: Performance of some stretchable conductors. (A) Stretch against normalized resistance of hydrogel, ITO, AgNWs, SWMTs and graphene. **(B)** Transmittance (at 550 nm) against sheet resistance of hydrogel, ITO, AgNWs, SWMTs and graphene (adapted from [36]).

Until recently, indium tin oxide (ITO) has been used on touch panels, however, it does not fill the requirements of biocompatibility or stretchability. On the other hand, hydrogels can be essential for the next generation of touch panels since they fulfil these demands. With this in mind, Kim *et al* [38] demonstrated a soft and stretchable ionic touch panel based on a polyacrylamide hydrogel containing lithium chloride salts. An epidermal touch panel was made with this hydrogel on top of a VHB^{TM} film used as an insulator and for better adhesion. The working principle of this touch panel was based on the change of current when a human finger touches on the ionic conductor. The epidermal touch panel was used to write words, play piano and some games [38]. Apart from display applications, the transparency of these materials is important to enable signals' transmission without optical interference [37].

Even more, conductive hydrogels combine with VHB^{TM} have been used to integrate strain and pressure sensors [37]. Based on a capacitive sensing, they showed an array of pressure sensors made with conductive hydrogels that could detect the locations and pressure of touch.

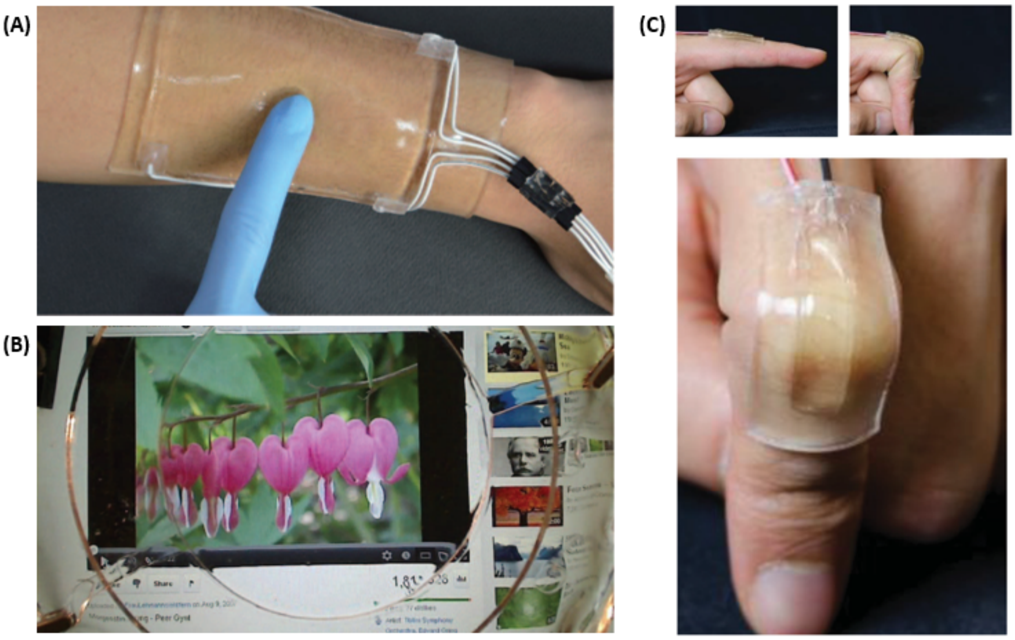

Figure 2.6: Examples of applications with conductive hydrogels: **(A)** epidermal touch panel [38], **(B)** transparent loudspeaker [36] and **(C)** strain sensor [37].

More applications have emerged in the last few year and based on the capacity of hydrogels, conductive or not, it will continue to appear new advantages combining different materials.

2.3 Hydrogel-PDMS hybrids

One very recent direction of research is hydrogel-elastomer hybrids. In most of the above referred examples of applications, it is possible to observe that a VHB$^{\text{TM}}$ tape elastomer is used to incorporate hydrogels. This adhesive layer protects the hydrogel from physical damage, reduces the water evaporation and improves the overall mechanical robustness of the conjunction. Nevertheless, these are not permanent conjunctions thus resulting in a weak interfacial bonding.

A hydrogel-elastomer hybrid is very attractive, not only because the elastomer allows protection of the hydrogel and mechanical robustness, but also because of the different range of application where elastomers can be applied to. For instance, most of the previous advances on stretchable electronics, microfluidics and lab-on-a-chip were based on elastomers, in particular PDMS was used as the substrate. Moreover, methods for integration of stretchable electronics on PDMS are rapidly advancing and promising.

Therefore, the overall goal of this dissertation is defined to explore and study how to combine advances in hydrogels and elastomer based electronics, in order to reach a novel generation of biomonitoring patches that can monitor several health indices and physiological conditions of the body. These patches that can analyse body chemical and physical events, and at the same time, keep the promise of being ultra-thin, light-weight, skin-like stretchable devices that are ergonomic and can stay on the skin for several days.

As previously described, both PDMS and hydrogels have singular properties that complement each other and make them suitable for the field of stretchable electronics for biomonitoring patches.

However, combinations of this two materials are not that common since the few developed exhibit low mechanical strength, weak interfacial bonding and patterning microstructures are not easy [19]. Most of the hydrogel-elastomer hybrids use VHB$^{\text{TM}}$ since it is an adhesive tape but it also has the same limitations as hydrogel-PDMS combinations. One of the reasons for this weak interface is that elastomers are permeable to oxygen, while oxygen inhibits the free-radical polymerization that forms the hydrogel network and can also difficult the covalent crosslinked between PDMS surface and the hydrogel. Additionally, the bonding of hydrogels to PDMS can be diminished by the recovery of hydrophobicity of functionalized PDMS surface

One breakthrough in this field was recently demonstrated in an article published in *Nature* [19], where researchers were able to make robust interfaces (interfacial toughness over 1000 J m^{-2}) between hydrogels and several elastomers, including PDMS. They developed a new methodology that integrates new improvements for the field of soft materials and provides a stretchable hybrid with high interfacial toughness. The method consists in using tough hydrogels in which a stretchy polymer network is formed that can dissipate energy under deformation and these tough hydrogels allow pre-shaped the hydrogel with its physical crosslinking. This way it is possible to pre-shaped both of elastomers and hydrogels before the bond, conserving their microstructures. Moreover, through a benzophenone modification of cured elastomer surface, it is possible to chemical anchoring the hydrogel to the elastomer and reduce the oxygen effect.

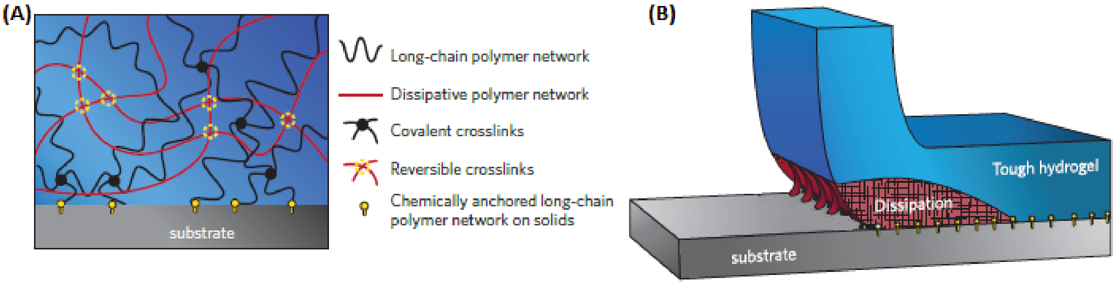
(A)
substrate
Long-chain polymer network
Dissipative polymer network
Covalent crosslinks
Reversible crosslinks
Chemically anchored long-chain polymer network on solids
(B)
Tough hydrogel
Dissipation
substrate

Figure 2.7: Bonding of tough hydrogels to the solid substrate. (A) Tough hydrogels are a combination of long-chain and mechanically dissipative polymer networks, which are chemically anchoring to the substrate surfaces. **(B)** The bond between tough hydrogel and the substrate have a high interfacial toughness that allows large deformation and mechanical dissipation in the hydrogel during detachment (adapted from [33]).

The interface of these robust hydrogel-elastomer hybrids was proven to maintain intact under uniaxial strain test, the hybrid breaks before any damage occur to the bonding. In comparison with a hybrid without benzophenone treatment, due to the weak interface, the tough hydrogel detaches from the elastomer under small deformation. Even when combined a common hydrogel on top of a treated elastomer, the hybrid can sustain high deformation until the debonding occurs and it propagates within the hydrogel leaving a residue layer on the elastomer surface. This behaviour empathizes the role of benzophenone treatment in order to achieve a robust interface between the hydrogel and elastomer. In addition, the use of tough hydrogel allows high stretchability and the dissipation of energy under deformation [19].

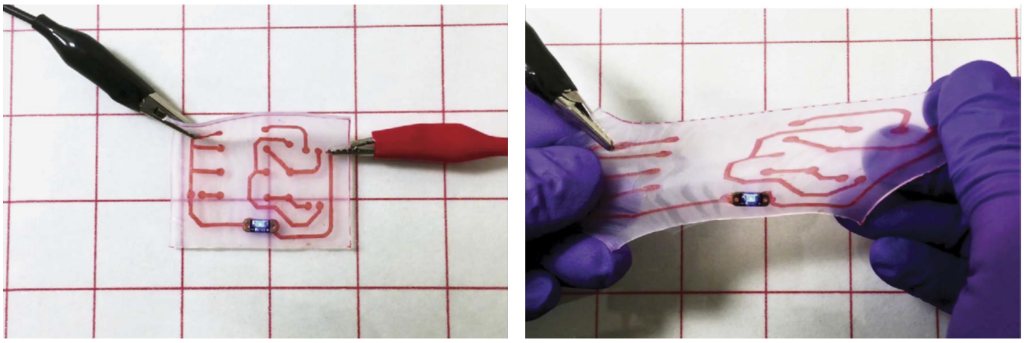

Figure 2.8: Conductive hydrogel circuit pattern on a elastomer. When connected to a AC power source it could light up a LED, even under deformation [19].

In order to demonstrate some applications, a microfluidic chip based on hydrogel–elastomer hybrids with micro-channels patterned on interfaces were developed. Moreover, a conductive hydrogel circuit pattern on an elastomer was used to light up a LED and even when repeatedly stretch the electrical resistance remained almost the same (figure 2.8) [19].

This advanced triggered new researchers, for instance, more recently devices based on these hydrogel-PDMS hybrid were developed for hosting programmed cells and to be used as living wearable devices to detect chemicals on the skin [39].

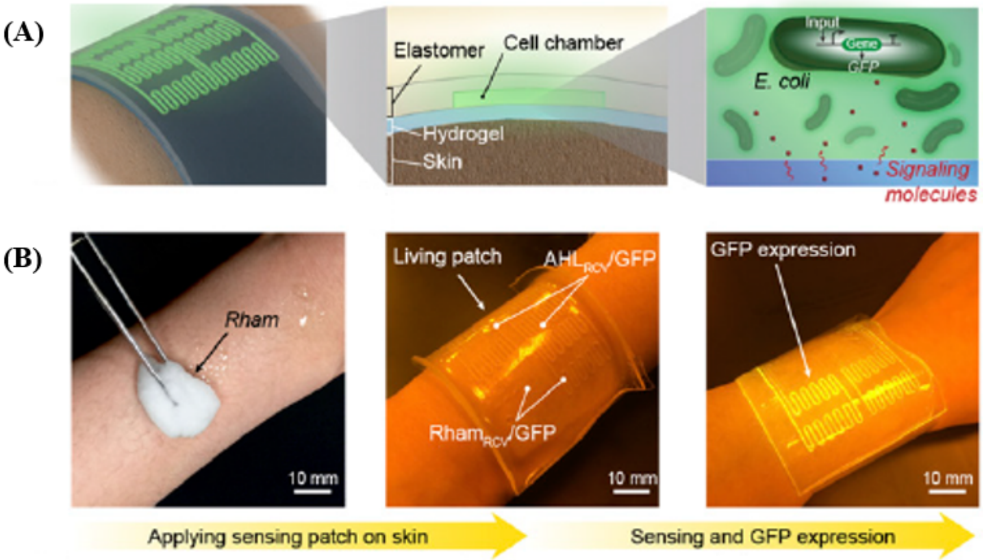
(A)
Elastomer
Cell chamber
Hydrogel
Skin
Input
Gene
GFP
E. coli
Signaling molecules
(B)
Rham
10 mm
Living patch
AHL_{RCV}/GFP
$Rham_{RCV}$/GFP
10 mm
GFP expression
10 mm
Applying sensing patch on skin
Sensing and GFP expression

Figure 2.9: Hydrogel-PDMS living patch.(A) On the wavy cell channels is placed engineered bacteria that can detect signaling molecules. (B) Example of the sensing mechanism with Rham solution. After detecting, the channels became fluorescent [39].

This progress on the fabrication of robust hydrogels-PDMS hybrids enables a great range of applications such as in microfluidic systems, tissue engineering and stretchable electronics. Integrating robust hydrogel-PDMS hybrid in the field of stretchable electronics for biomonitoring allows the development of tough patches with high stretchability and good interface with the human body.

Chapter 3

Materials and methods

In this chapter, the materials and fabrication methods are presented. Stretchable materials as PDMS and hydrogels are characterized, followed by EGaIn and FPCBs description. The fabrications methods and performed tests are also described in this section.

3.1 Materials

3.1.1 Hydrogels and tough hydrogels

Hydrogels

Hydrogels consist on a crosslinked hydrophilic polymeric network that can imbibe and hold large quantities of water without structural alterations. This ability is a result of the presence of hydrophilic groups such as amino, carboxyl and hydroxyl which form the network [31]. Hydrogels can be classified based on their chemical composition, properties, preparation, origin, responses to the environment and by their crosslinking type [31, 40]. The monomers that constitute the network can be bond through chemical crosslinks which are a permanent junction or physical crosslinks as entanglements, crystallites or ionic interactions, leading to two different types of hydrogels respectively [31].

Tough Hydrogels

Tough hydrogels are a recently reported class of hydrogel that present high stretchability since they consist of a covalently crosslinked polymer network and physically crosslinked dissipative polymer network [33]. Considering that most of the hydrogels are not highly stretchable this new development can exceed some of their limitations.

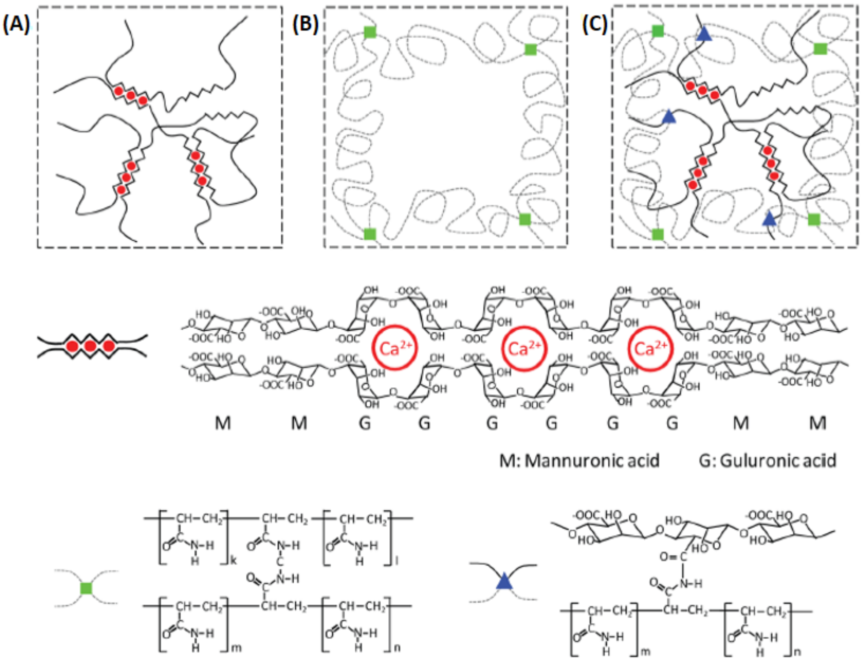

Figure 3.1: Polymer networks of three types of hydrogels: (A) Alginate hydrogel, physically crosslinked through G blocks and Ca^{2+}. **(B)** Polyacrylamide hydrogel, that is covalently crosslinked with a crosslinking agent (MBAA). **(B)** Polyacrylamide-alginate hybrid, forming a tough hydrogel (adapted from [41]).

The presences of physical crosslinks allow the pre-shaping of the hydrogel to a desired microstructure [19]. This reversible crosslinking enables the dissipation of mechanical energy under deformation through chain scission [33]. Furthermore, the chemical crosslinking is responsible for the toughness and acts like a memory of the initial state. Besides, the long-chain network enables the chemical anchoring to solid surfaces [41]. Therefore, the combination of the physical and chemical crosslinking allows us to obtain a stretchy polymer network that can dissipate easily mechanical energy.

In order to achieve the highest stretchability, in this work PAAm-alginate tough hydrogels are prepared. For the chemical crosslinking network acrylamide (AAm; TCI) is used as the monomer, N, N'-methylenebisacrylamide (MBAA; Riedel-de Häen) as the crosslinking agent and 2-Hydroxy-4'-(2-hydroxyethoxy)-2-methylpropiophenone (Irgacure 2959; Sigma-Aldrich) as the photoinitiator. For the ionic crosslink, sodium alginate (PanReac AppliChem) and calcium sulfate dihydrate (Fluka) are used.

3.1.2 PDMS

Polydimethylsiloxane (PDMS Sylgard® 184 from Dow Corning Corporation) is a silicone based elastomer widely used for the fabrication of Micro Electro Mechanical Systems (MEMS). It is a highly transparent polymer that can be used as a dielectric, since as its pure state is not conductive. PDMS is commercially available in two parts: silicone base elastomer and a curing agent. It is usually obtained by mixing both parts in a 10:1 weight ratio.

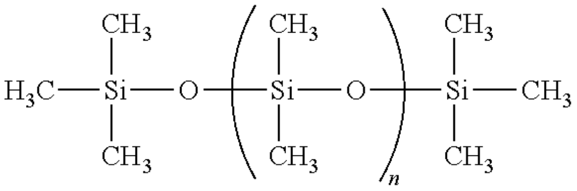

Figure 3.2: Chemical structure of PDMS.

Besides its low cost and easy manufacturing, PDMS exhibits others attractive properties as it is chemically inert, stable in different environment, mechanically robust and permeable to gases, including oxygen [19,42]. There is a great versatility in applications, for example, PDMS has been applied on microfluidic devices for biomedical applications, microfluidic devices (microreactor, microchips for capillary gel electrophoresis and hydrophobic vent valves [43]. Moreover, PDMS is non-toxic and biocompatible which make it possible to use them as biomaterials in catheters, implants insulation for pacemakers and ear and nose implants [42]. However, its strong hydrophobicity can sometimes limit its use.

3.1.2.1 Surface Modification of PDMS

Since PDMS surface is highly hydrophobic, a surface modification is needed so it can adhere to hydrogels that contain high water content. Moreover, as previously described PDMS is highly permeable to oxygen that inhibits the free-radical polymerization that occurs on hydrogels, when combining hydrogels with PDMS. In order to eliminate this oxygen effect and achieve a robust bond on the hydrogel-PDMS hybrid, a surface modification on PDMS is essential.

The most commonly used surface modification technique is surface activation with oxygen plasma. This technique relies on the production of reactive species that attack the backbone of PDMS and creates silanol functional groups on its surfaces [44]. However, the modification is not permanent since minutes later PDMS surfaces recover its hydrophobicity and it can induce undesirable surface cracks [26].

A powerful modification is graft photopolymerization, a chemical modification that allows local grafting monomers to PDMS surface using UV radiation [45]. Benzophenone (BP) can be used as a photoinitiator since in the presence of ultraviolet (UV) light it produced a triplet state that can abstract hydrogen atoms from methyl groups on PDMS surface, which produce radicals. This enables grafting of monomers on the PDMS surface with changing its bulk properties [45]. Besides, the benzophenone acts as an oxygen scavenger thus removing the oxygen effect. The graft polymerization process is divided into two steps: first, apply benzophenone solution on the target surface and BP diffusion into the polymer matrix happens; second, place functional monomer solution on the surface and graft photopolymerization will start with UV light exposure. This modification is advantageous since benzophenone is soluble in various organic solvents. Also, a chemical and mechanical robustness is achieved [45].

Therefore, in this work, a benzophenone solution (in ethanol) is used to modify the PDMS surface in order to allow chemically anchoring of the hydrogel onto the surface of PDMS and to eliminate the oxygen effect.

3.1.3 Liquid Metal - EGaIn

There exist some metals that are liquid near room temperature, which make them interesting to soft electronics and microfluidic systems. Due to its liquid state, when under deformations liquid metal can adapt in the microchannels maintain conductivity. The most known liquid metal is mercury. However, as mercury is toxic it should be avoided. A substitute to mercury is gallium-based alloys since it has a low bulk viscosity, low toxicity, high electrical and thermal conductivity [28, 46]. The more popular gallium alloys are Galinstan (alloy with Gallium, Indium and Tin) and EGaIn (74.5 wt.% of Gallium and 25.5 wt.% of Indium). Within these two, EGaIn is most commonly used gallium-based alloy since it has the highest electrical conductivity [28].

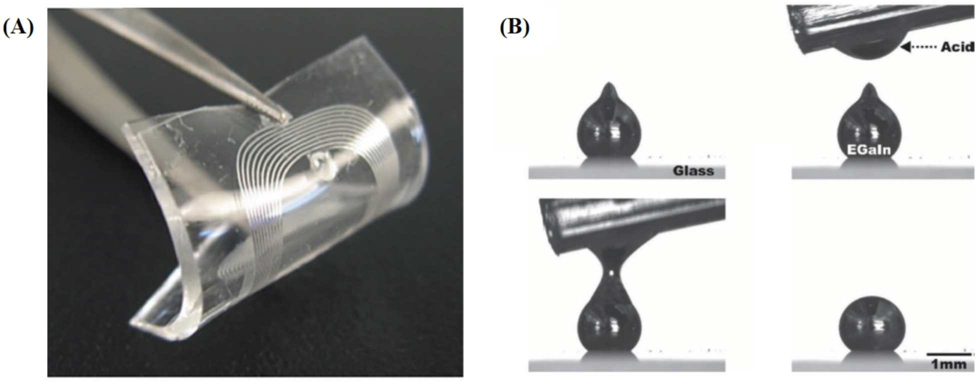

Figure 3.3: Liquid metal alloys enable the fabrications of stretchable circuits.(A) Stretchable circuits with liquid metal [46]. **(B)** EGaIn forms an oxide layer in the presence of oxygen that stabilises the metal into none-equilibrium shapes. When exposed to acid, the oxide layer is removed and the metal beads up [28]

.

In the presence of oxygen, gallium forms a thin oxide layer on its surface which mechanically stabilizes it in stable, non-equilibrium shapes. Thus, the oxide layer allows patterning by many conventional techniques, for example, screen/stencil printing, injection, contact printing and spray painting [28]. This oxide skin also improves the metal adhesion to surfaces [46]. Liquid metal has been used to create stretchable systems in different shapes, such as wires, interconnects, antennas and electrode [46]. Moreover, EGaIn was combined with conductive hydrogels to produce soft devices as memristors [47] and diodes [48]. Both of these devices are composed of two EGaIn electrodes and two hydrogels with polyelectrolytes (polyacrylic acid, PAA and polyethyleneimine, PEI). Here a good interaction between each hydrogel and EGaIn was observed.

3.1.4 Flexible PCB

Flexible printed circuit boards (FPCBs) consist on a thin flexible foil (polyimide, polyester or Kapton) covered by a thin film of copper that can be fabricated with standard photolithography and wet-etching methods. Despite its flexibility, FPCBs are not stretchable. They can be used as an interface material between the stretchable and rigid components. When in contact with cooper, EGaIn has the ability to alloy creating a solid layer on the copper surface, which is important to maintain conductivity under deformation [49].

3.2 Fabrication Methods

3.2.1 Fabrication of hydrogel-PDMS hybrid

The hydrogel-PDMS hybrid fabrication method is based on the process developed by Yuk *et al* [19] described in the previous chapter.

The hybrid consists of a 1 mm layer of PAAm-alginate tough hydrogel chemical anchored to a 1 mm layer of PDMS (figure 3.4). As already reported, the tough hydrogel is used to achieve a higher stretchability and to enhance the mechanical properties when compared to the common hydrogel. A benzophenone solution is used to modify the surface of PDMS, in order to accomplish a high interfacial toughness between these two materials.

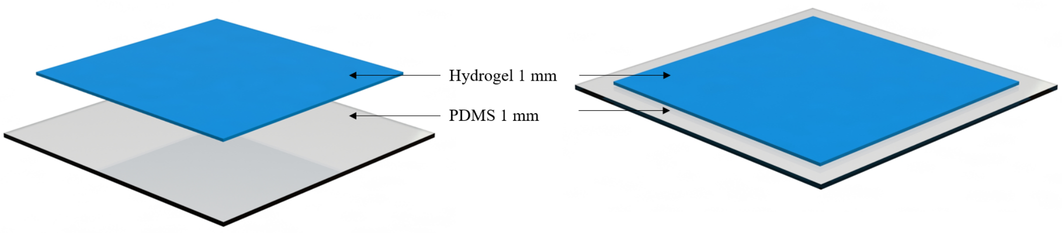

Figure 3.4: The hybrid structure.

The fabrication method can be divided into three main steps: preparation of the PDMS, preparation of the hydrogel and hydrogel-PDMS assembling.

1. PDMS preparation

The PDMS is prepared by mixing the elastomer base with the curing agent by a 10:1 weight ratio and with a thin film applicator, the PDMS layer is cast on a glass substrate. In order to avoid bubbles, it is applied vacuum for 10/15 minutes and then the PDMS is cured at 100 °C for 30 minutes.

Once the PDMS layer is cured and before applying the benzophenone treatment, the cured PDMS surface is cleaned with deionized water and methanol, and completely dried with compressed air. The entire surface is covered with a benzophenone solution (10 wt.% in ethanol) for 2 min at room temperature. Thereafter, the PDMS is washed three times with methanol and thoroughly dried with nitrogen gas. The application of this surface treatment is only done before the assembling with the hydrogel.

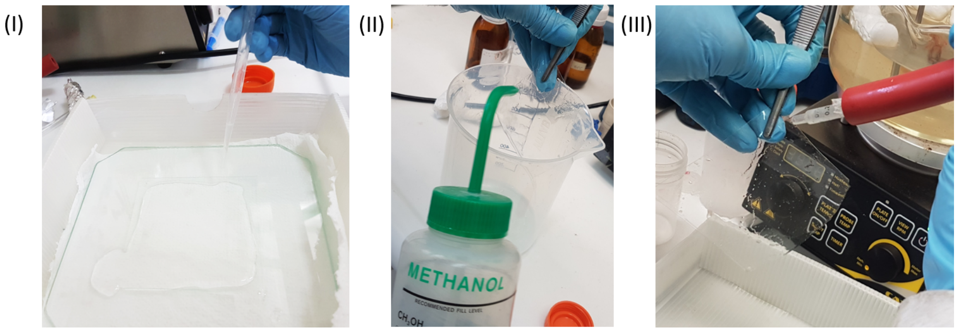

Figure 3.5: Surface modification of cured PDMS surface. (I) A benzophenone solution is applied over all surface. (II) After 2 minutes, the surface is washed with methanol and (III) dried with nitrogen gas.

2. Hydrogel preparation

The preparation of hydrogel and the assembling with the PDMS are both done very carefully since the presence of oxygen inhibits the polymerization process and the chemical bonding to the PDMS surface. To avoid this oxygen effect, the processes involving hydrogel solutions are done with syringes and nitrogen gas.

Table 3.1: Composition of the tough hydrogel with 85 wt.% of water.

Component	Concentration
Acylamide (AAm)	12.05 wt.%
N,N-methylenebisacrylamide (MBAA)	0.017 wt.%
Sodium alginate	1.95 wt.%
Calcium Sulfate	20 x 10^{-3} M
Irgacure 2959	0.2 wt.%

Given the concentration presented on table 3.1, a pre-gel solution containing AAm, MBAA and sodium alginate is prepared and degassed. Thereafter, 5.8 ml of this degassed solution is transferred to a syringe. The degassing process is done by first applying vacuum to the solution and then introducing nitrogen gas. The Irgacure 2959 and the calcium sulfate are introduced directly into another syringe (table 3.1). A few drops of water bubbled with nitrogen are added through the tip of the syringe in order to fill the space between the powders. The two syringes are connected with an adaptor at their tip and the solutions are quickly mixed inside them in order to avoid entrance of oxygen.

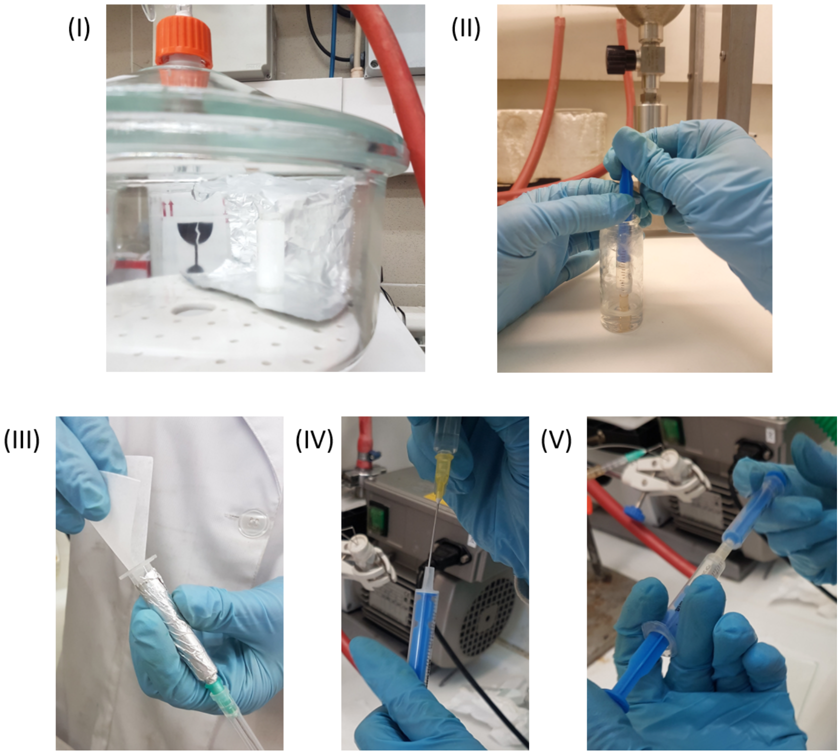

Figure 3.6: Hydrogel preparation. (I) After degassed the pre-gel solution, (II) the solution is pulled to one syringe. (III) In another syringe, calcium sulfate and irgacure 2959 are introduced and thereafter, (IV) some drops of water bubbled with nitrogen gas are added on the tip of this syringe. (V) The two syringes are connected and the solutions are mixed.

3. Hydrogel-PDMS assembling

Right after mixing the solution and application of the benzophenone treatment over the cured layer of PDMS, the hydrogel is poured over a mould made by glass slide with a rubber frame (figure 3.7), carefully covered by the treated PDMS and finally by a glass slide. This assembling process is done with a continuous nitrogen flow. This hybrid is kept for 20 minutes in nitrogen to allow the physical crosslink and then for 1 hour in a UV chamber in order to enable the chemical crosslink and the chemically anchoring of the hydrogel to the PDMS surface.

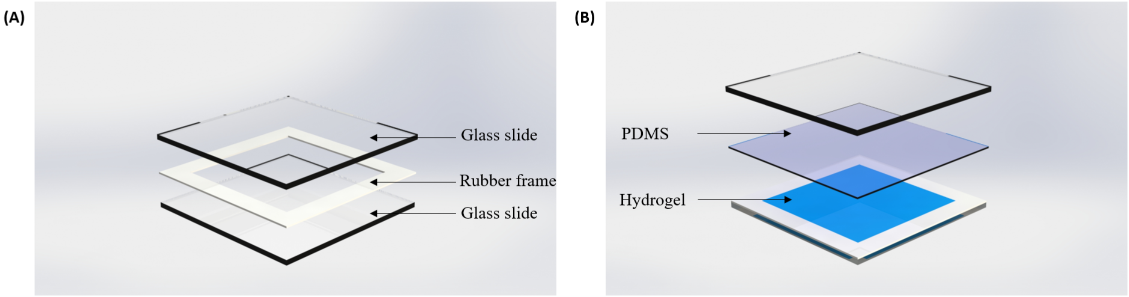

Figure 3.7: (A) The mould used to developed the hydrogel-PDMS hybrid. With the help of silicone grease, the rubber frame is sealed on top of a glass slide. The inner rectangular on the rubber frame has 70x70x1 (length x width x thickness). (B) The assembling of the hydrogel and treated PDMS on the mold.

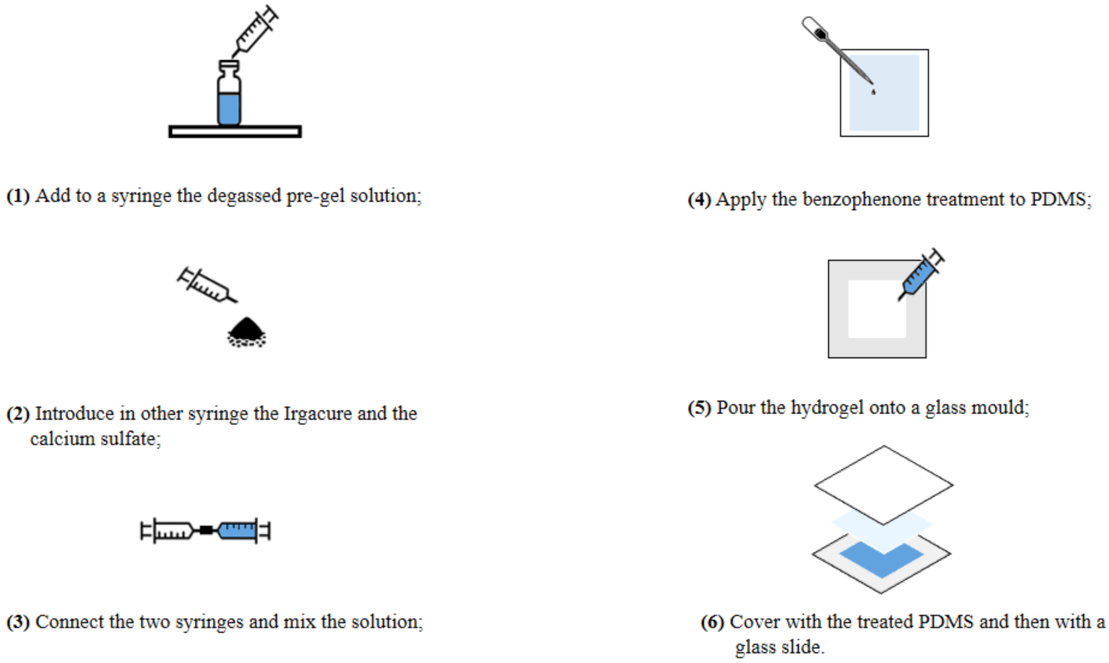

(1) Add to a syringe the degassed pre-gel solution;

(2) Introduce in other syringe the Irgacure and the calcium sulfate;

(3) Connect the two syringes and mix the solution;

(4) Apply the benzophenone treatment to PDMS;

(5) Pour the hydrogel onto a glass mould;

(6) Cover with the treated PDMS and then with a glass slide.

Figure 3.8: Resume schematic of the fabrication process of hydrogel-PDMS hybrid.

After the successful conjunction between PDMS and hydrogel, we would then explore how this can be used for a bio-monitoring patch. The actual bio-monitoring patch development is not the goal of this dissertation. Rather, the objective is to explore if it is possible to combine a stretchable circuit developed over PDMS with hydrogel-PDMS electrodes. While hydrogel provide an excellent match with the human skin, and PDMS provides an excellent substrate for stretchable MEMS and microfluidics, their combination is attractive. As a case-study, we opted to show an EMG circuit for detection of muscular activities. The reason EMG was chosen, was simply because of the previous experience of the group in this field as well as available hardware and software for signal acquisition and processing.

3.2.2 Fabrication of a soft EMG sensor

A soft EMG was developed in order to demonstrate the applicability of hydrogel-PDMS hybrid on wearable biomonitoring patch. Two EMG sensors with different shapes of electrodes were designed: square and round electrodes, in which the fabrication process was exactly the same.

The basic design is presented in figure 3.9. For the sensing electrodes, the hydrogel-PDMS hybrid is used, with the hydrogel as skin interface. Thin PDMS layers are fabricated by a thin film applicator to support the electrodes and embed the conductive connections.

Based on the reported good interaction between hydrogel and EGaIn [47,48], the liquid metal is used for the circuit. Also, since EGaIn and copper have high affinity, adding to the fact that FPCBs are flexible and solve the mismatch between stretchable and rigid parts, these are chosen as a reliable interface.

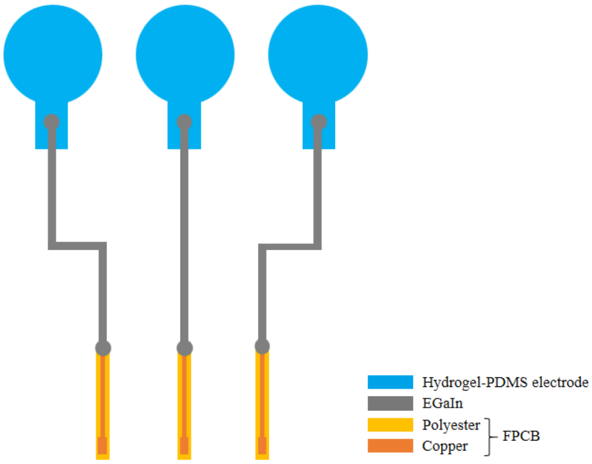

Figure 3.9: The design used to create the soft and stretchable EMG sensor onto PDMS layers.

3.2.2.1 Hydrogel-PDMS electrodes

Once the hydrogel-PDMS hybrid is made, the desired shape of the electrodes is created through a laser cutting system (CO_2 laser, Universal Laser Systems®, 10.6 μm wavelength, 30 W) with vectorial mode 35% power, 5% speed and 1000 Point Per Inch (PPI). In order to have the hybrid in a flat position for the laser cut, the hybrid is covered with adhesive tape on top of an acrylic surface.

To induce the required ionic conductivity, the electrodes are submerged in a sodium chloride solution (concentration of 3 M) for 6 hours, based on the initial method of Yuk *et al* [19]. The conductivity is only introduced after the laser cut to avoid burns around the electrodes.

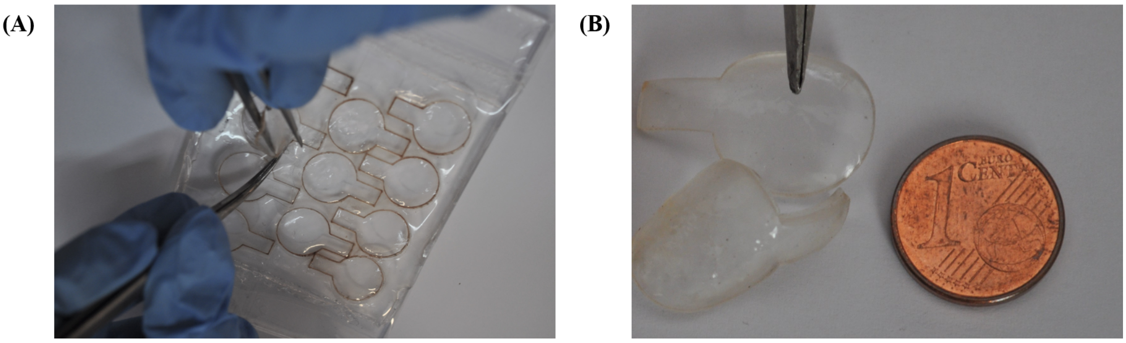

Figure 3.10: Hydrogel-PDMS electrodes. (A) The hydrogel-PDMS hybrid is cut to the required shape using a laser cutting system. **(B)** After introducing conductivity, the thickness of the electrodes slightly increases. They have 15 mm of diameter.

3.2.2.2 Stretchable circuit and interface

The fabrication method of the stretchable circuit and interface is based on a new multilayer method being developed in ISR labs.

The method consists on applying a multilayer interface which uses a buried Vertical Interconnect Access (VIA) as a connection between two layers of conductive materials. This technique allows the fabrication of multilayer systems where the liquid metal circuit can be connected through VIAs to FPCBs or hydrogels in different layers.

The general procedure consists on the following essential steps: integration of FPCBs, integration of hydrogel-PDMS hybrid electrodes and VIAs and circuit fabrication.

1. Integration of FPCBs

The FPCBs are placed on a half-cured layer of PDMS (200μm) with the copper facing down to the PDMS in order to allow the fabrication of the VIA. To facilitate the placement of the FBCBs and the electrodes, a laser pattern stencil is used as a guide on the other side of the glass slide.

2. Integration of hydrogel-PDMS hybrid electrodes

Once the first layer is cured, a new layer of PDMS (200μm) is added to cover the FPCBs and when half-cured the hybrid electrodes are introduced. After cured, filaments of PDMS are poured around the electrodes to improve the adhesion onto the PDMS layers.

3. VIAs and circuit fabrication

In the basic design there are two types of VIAs: the ones used to access the conductive hydrogel and the others to access the copper on the FPCBs. Both of them are laser printed (rastering mode, 50% power, 80%speed and 500 PPI) through the PDMS until it reaches the desire substrate. These VIAs are created from the opposite layer where the hydrogel electrodes are placed, for these purpose the system has to be flipped over before laser ablation. The depth of the access is controlled by the number of repeated ablations in the same position, while maintaining the same parameters for both VIAs. For the hydrogels' VIAs 14 prints are needed and for the copper only 2 are required.

The VIA is achieved by liquid metal depositing inside the printed vertical access space. A laser patterned stencil is used to fill the VIAs and fabricated the circuit. Both are sealed with a thin layer of PDMS resulting on a total thickness of 2700 μm.

Once the last layer of PDMS is cured, the hydrogel electrodes are again submerged into the sodium chloride solution since during the fabrication process high temperatures are used and the water from the hydrogel evaporates.

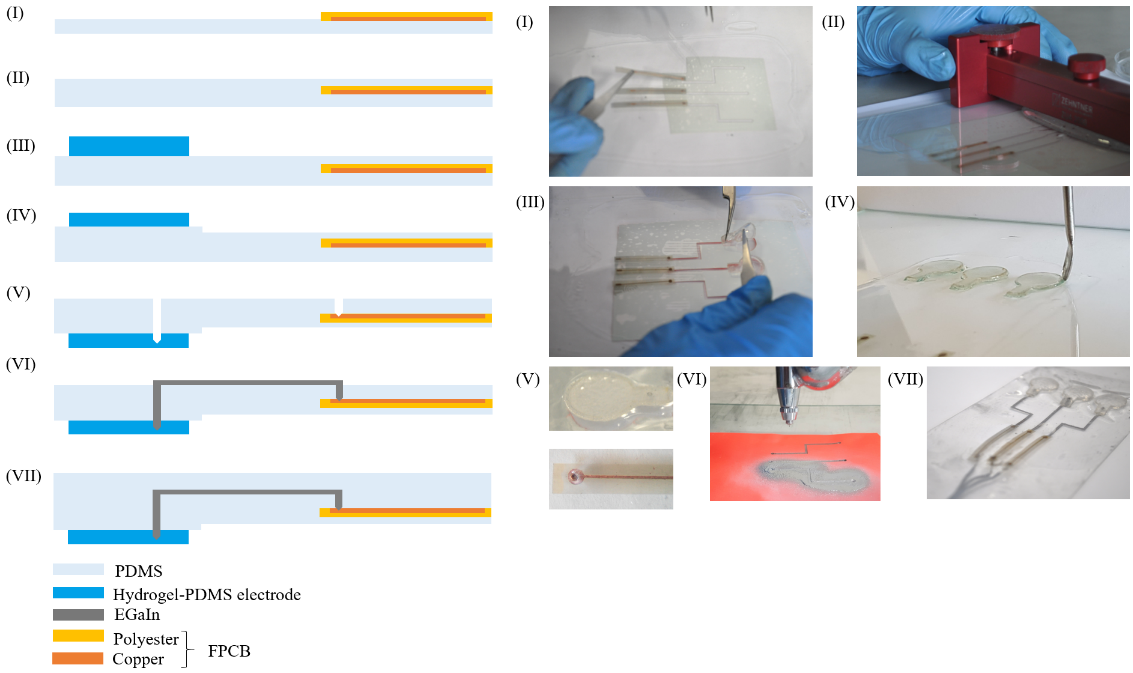

Figure 3.11: Schematics and respective photos of the fabrication method of the soft EMG. (I) Place the FPCBs on a half-cured PDMS layer. (II) Cover with another PDMS layer. (III) When this last layer is half-cured, place the hydrogel-PDMS electrodes. (IV) Pour small filaments of PDMS around the electrodes. (V) Fabricate the hydrogel and copper VIAs. (VI) Spray-deposit of liquid metal. (VII) Seal with a layer of PDMS.

3.2.3 Fabrication of GSR sensor

The galvanic skin response represents the variation of the electrical properties of the skin in response to sweat secretion [11]. As hydrogels are mostly composed of water and are permeable to biological fluids, such as sweat, they appearer to be an excellent choice for GSR electrodes.

Therefore, in order to test hydrogel-PDMS electrodes for GSR measurements and with the same fabrication process used for the soft EMG, a GSR sensor was developed. In this sensor, the measurements of the galvanic skin response are done between two hydrogel-PDMS electrodes. This way, in contrast to the EMG sensors, the GSR sensor only has two electrodes.

3.3 Experimental tests

3.3.1 Dehydration test

With the aim to study the water loss of the hydrogel-PDMS hybrid, we conducted a dehydration test. Two samples with 3x1 (length x width) were prepared from the hydrogel-PDMS hybrid, through laser cutting and then they were made conductive with the sodium chloride solution (3 M) for 6 hours. One of the samples was left in ambient air at room temperature and the other placed over the skin with an adhesive tape. The weight loss of both the samples was registered during 76 hours.

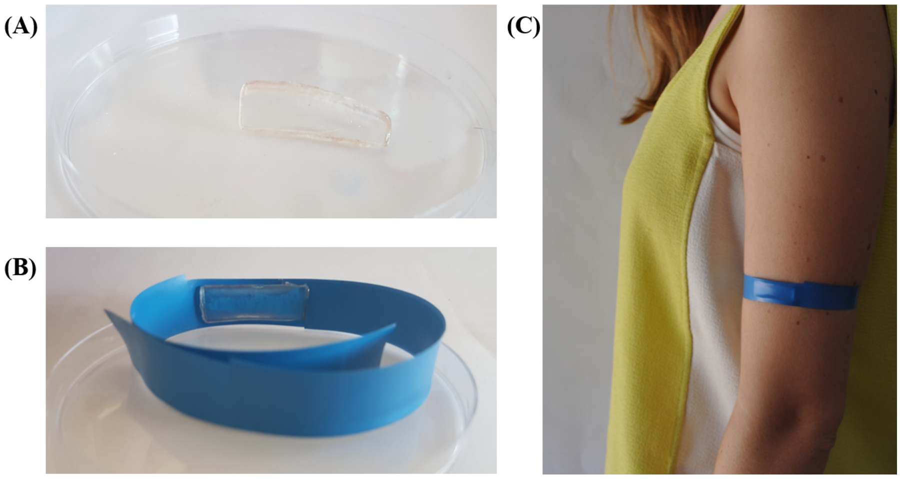

Figure 3.12: Dehydration test: **(A)** sample left in air ambient and **(B), (C)** sample used over the skin.

3.3.2 Impedance Analysis

The performance of electrodes used to measure biopotentials depends on the electrode-skin impedance. An ideal electrode has low electrode-skin impedance resulting in a high biological signal quality and low noise. Following this logic, a high electrode-skin impedance leads to low quality of the biological signal since there is a bigger hindrance to the transmission of the biopotential [50].

According to the model proposed by Albulbul *et al* [50], the equivalent circuit model of the electrode-skin interface is shown at the figure 3.13(**A**). As the electrodes used were identical, the components values on the first electrode are the same as on the second electrode. Moreover, as the impedance of a healthy human arm exhibits a low value when compared to the electrode-skin impedance, it can be neglected, resulting on the following equivalent circuit model.

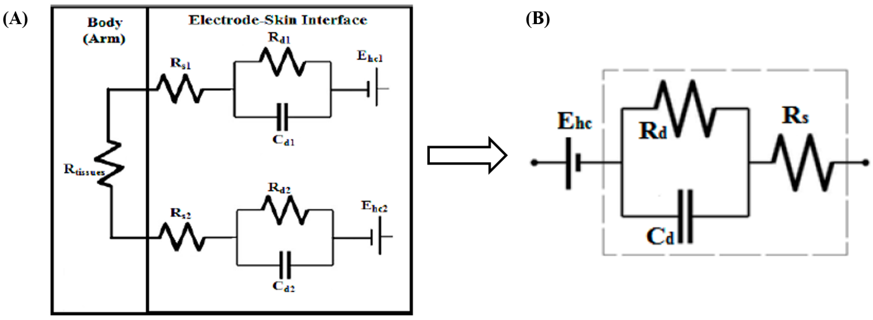

Figure 3.13: **(A)** Diagram of the electrodes system. **(B)** Equivalent circuit model of the electrode-skin impedance [50].

On the equivalent circuit model for the electrode-skin impedance figure 3.13(**B**), the component:

- E$_{hc}$ represents the potential difference that is generates between the skin or electrolyte (gel or sweat) and the electrodes from the ions in that area;
- C$_{d}$ is the capacitance originated from the moving charges between skin double layer and the electrode;
- R$_{d}$ is the resistance to the movement of the charges between the electrode and the skin;
- R$_{s}$ is the sweat or electrolyte gel resistance.

The impedance of the electrode-skin interface depending on the frequency is given by the following formula:

$$Z_e = R_s + \frac{R_d}{1 + j2\pi f C_d R_D} \tag{3.1}$$

where f is the frequency (Hz).

With the aim to compare the performance of some of the biopotential electrodes an impedance analysis was conducted. A diversity of electrodes were tested, some of them under development on the ISR labs. Besides the hydrogel-PDMS electrodes developed in this dissertation, silver/silver chloride (Ag/AgCl) and stainless steel electrodes were tested. Moreover, cPDMS electrodes made with carbon doped PDMS and zPDMS electrodes based on PDMS combination with silver-nickel particles oriented on the z-axis. Tattoo electrodes composed by silver ink alloyed with liquid metal on a temporary tatto paper substrate.

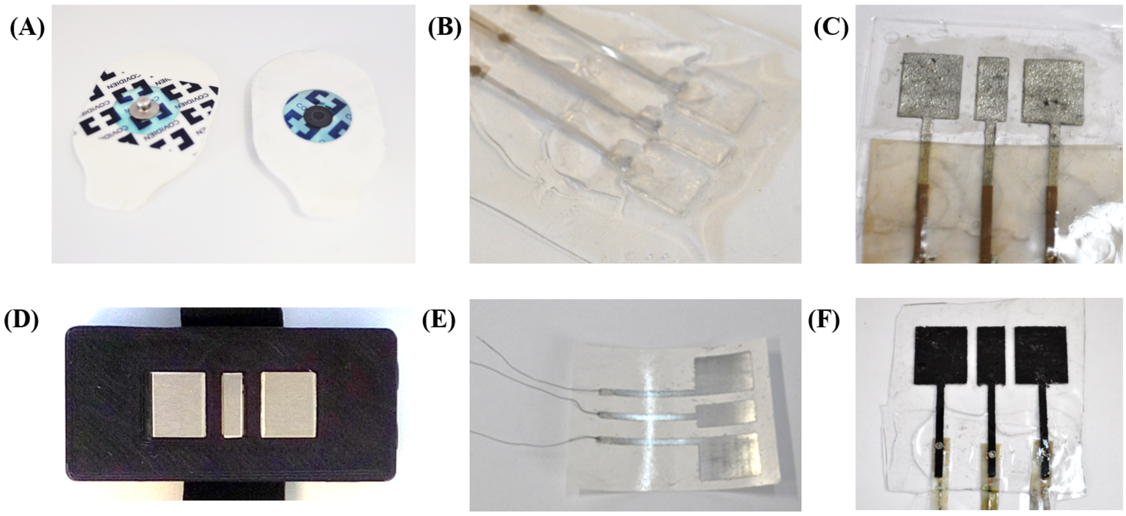

Figure 3.14: Electrodes used in the impedance measure test: **(A)** Ag/AgCl electrodes, **(B)** Hydrogel-PDMS electrodes, **(C)** zPDMS electrodes, **(D)** Stainless steel electrodes,**(E)** Tattoo electrodes and **(F)** cPDMS electrodes.

Experimental set-up

An impedance measurement system was used in which the response of the impedance to different frequencies when applied a low alternating electrical current was registered. For this propose, a precision impedance analyser (Agilent 4294A) was used with a 200 μA AC current, value that does not harm the human body. The impedance was measured from 40 Hz to 5 MHz (with 425 points).

Since the electrode-skin impedance changes from one person to another and from one part of the body to another [50], all tests were performed on the same subject and on the same body part. The electrodes were placed on the ventral side of the right forearm and had approximately the same distance between them.

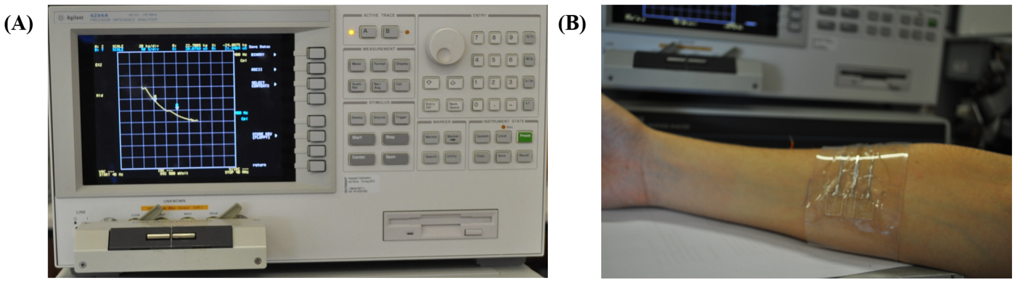

Figure 3.15: **(A)** The precision impedance analyser used. **(B)** Hydrogel-PDMS electrodes placed on the subject ventral side of the right forearm.

3.3.3 Soft EMG - signal acquisition

In order to evaluate the ability to detect muscular activity, the sensors made with hydrogel-PDMS electrodes were tested. The EMG sensor with the round electrodes was used for the detection of the flexor carpi radialis muscle movement and the EMG with the square hydrogel-PDMS electrodes for the flexor carpi ulnaris (figure 3.16). All recorded signals were compared to the signal from the stainless steel electrodes for the same movements and placed on the same muscle. Three movements were performed for each sensor: fist clenching, wrist flexion and opening the hand.

The acquisition system was developed in ISR labs, including the circuit board and the software appropriated for EMG recording.

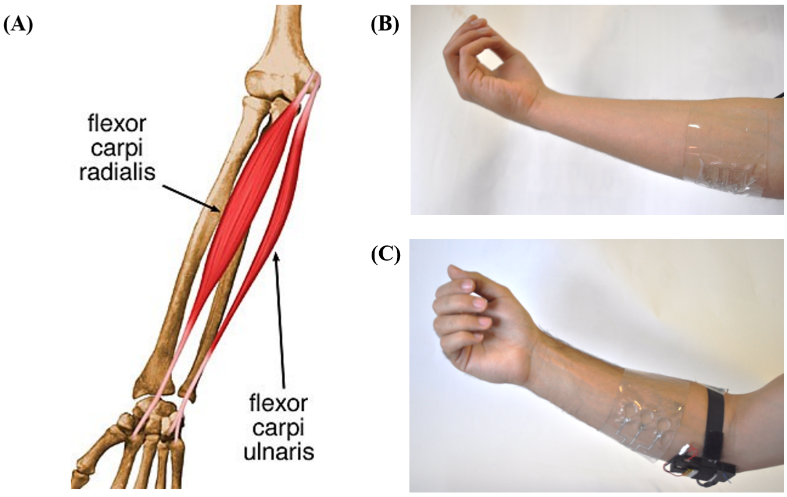

Figure 3.16: **(A)** Image of the position of flexor carpi ulnaris and the flexor carpi radialis muscles on the upper-arm [51]. The soft EMGs developed were used to detect the **(B)** flexor carpi ulnaris muscle and the **(C)** flexor carpi radialis muscles.

3.3.4 GSR measurement

With the aim to test hydrogel-PDMS electrodes for detection of changes on skin conductance, a GSR system was developed. This system allows the recording of skin resistance at each 130 ms. The measurements were taken by applying a voltage of 1 V (at 1 kHz) between two hydrogel-PDMS electrodes and acquired and processed by a microcontroller.

Usually, the GSR measurement is done on the hands or feet, since these areas have a higher concentration of sweat glands [10]. However, placing electrodes on this area can limit daily movements. In this work, the electrodes were placed on the left upper-arm with the help of an armband, which does not interfere with the routine.

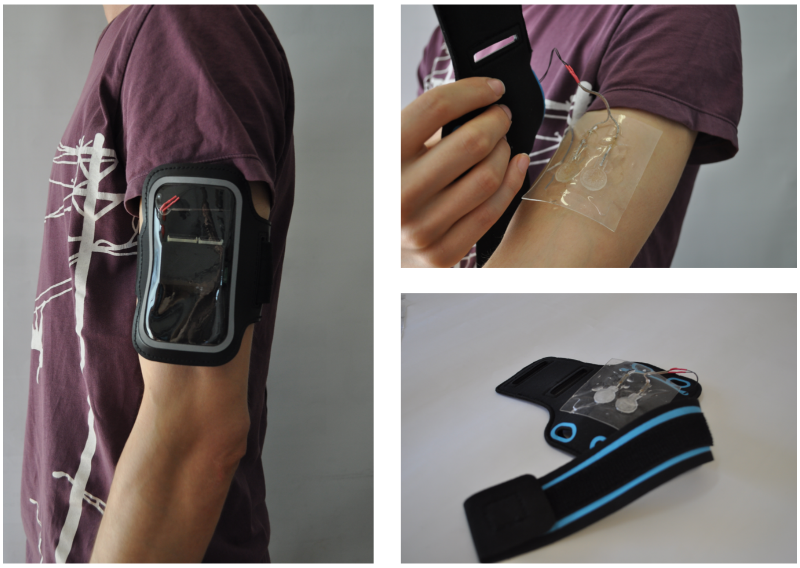

Figure 3.17: The GSR system was placed on the upper-arm of the subject and fixed with an armband.

Three different tests were conducted and all these tests were performed on the same healthy (23 years old male) volunteer.

In order to verify the efficiency of the skin resistance measurements for the hydrogel-PDMS electrodes, a comparison test was performed between these electrodes and stainless steel electrodes. The measurements were done during approximately 50 minutes under the same conditions. This test consisted on a static test since the subject was doing his daily activities.

Since during physical activities the sweat secretion increases, then the skin resistance is expected to decrease. To tested the developed sensor in detecting this changes, the subject wore the GSR sensor on his upper-arm while cycling back home (approximately for 45 minutes).

Moreover, to evaluate if the proposed sensor could detect changes of the skin resistance caused by stressful situations, the subject was submitted to different sonorous stimuli while listening to meditation music in a relaxed environment at a seated position, based on previous works [11]. Even more, two trailers of horror movies were presented.

Chapter 4

Results

In this chapter, the results obtained based on the fabrication methods and the experimental tests described in the previous chapter are presented.

4.1 Tough Hydrogel-PDMS hybrid

The result of the hydrogel-PDMS conjunction is a tough and stretchable hybrid. When pulled off from the mould the hybrid was easily removed without any damage, supporting the previous work developed, since it exhibits a tough interfacial bonding.

Because of the difference in Young's modulus of hydrogel (29 kPa [41]) and PDMS (between 360 and 870 kPa [52]), it is possible to observe a slight curvature on the hybrid.

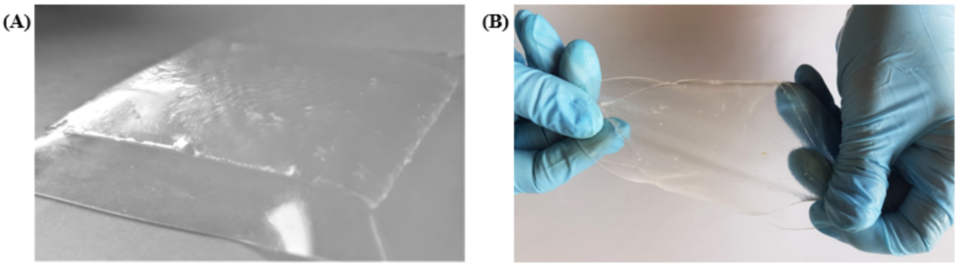

Figure 4.1: **(A)** Hydrogel-PDMS hybrid. **(B)** This hybrid is tough and can sustain high deformation.

4.2 Dehydration test

In this test, the water loss of two hybrid samples was registered: one attached to a subject arm and the other left in air ambient. As expected, the sample in contact with the body, lost water much slower than the hybrid sample left in contact with the air. In the plot from figure 4.2, it is possible to observe the weight ratio loss over the dehydration time. It can be seen in this plot that the air sample lost drastically water in the first 10 hours, reducing its total weight to almost half. On the contrary, the arm sample lost the water gradually.

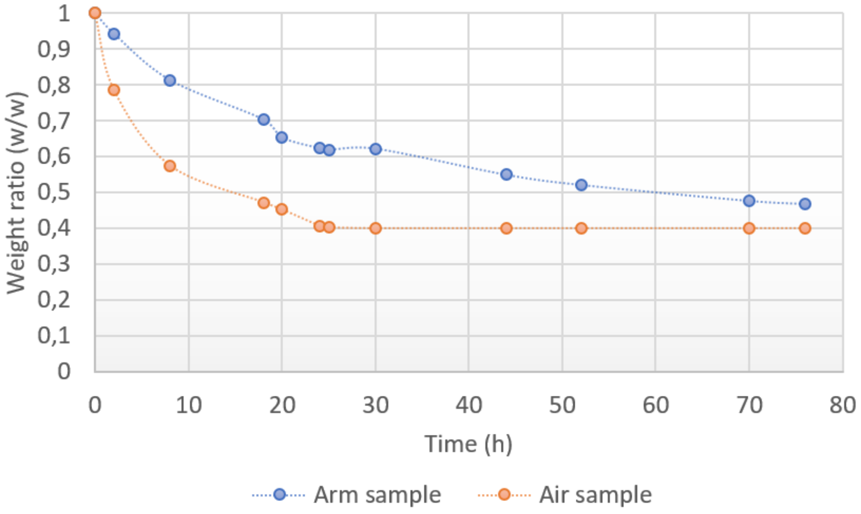

Figure 4.2: Weight ratio loss over dehydration time for both samples.

The water lost on the sample in contact with the body appears to happen through the borderlines of the hydrogel-PDMS hybrid since this parts are not completely in contact with the arm (figure 4.3). The area that was directly in contact with the skin does not have the same aspect as the borderlines, leading to the assumption that the water from this area diffused to the borders and then evaporated or it is absorbed by the body. This suggested that if we use a substrate that totally covers the hydrogel-PDMS from the outside layer, the dehydration process could be even more retarded. Moreover, the dehydration rate depends on the health and hydration status of the subject.

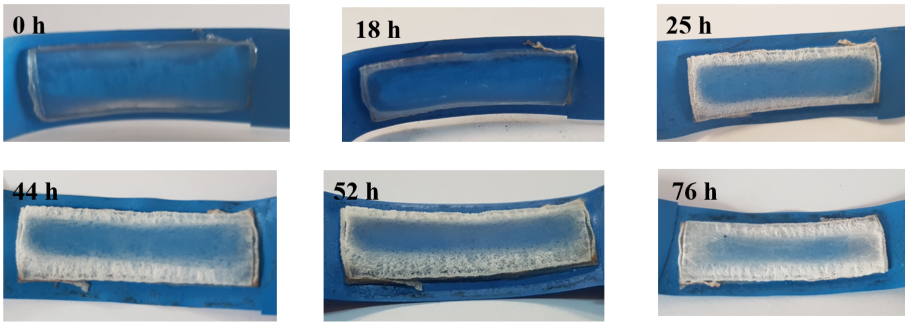

Figure 4.3: Photos of the hydrogel–elastomer hybrid sample in contact with the skin during the dehydration time.

4.3 Impedance analysis

In order to compare the electrode-skin impedance for different electrodes, using an impedance measurement system the response of the impedance to different frequencies was obtained for each pair of electrodes. As each pair of electrodes is equal, the impedance values are divided by two to determine the impedance for a single electrode.

The values of the circuit model components (figure 3.13) were determined by applying a least squares nonlinear curve fitting method in MATLAB to the Bode plot. In the Bode plot the impedance in function of the frequency is represented, for the each electrode (figure 4.4) [50].

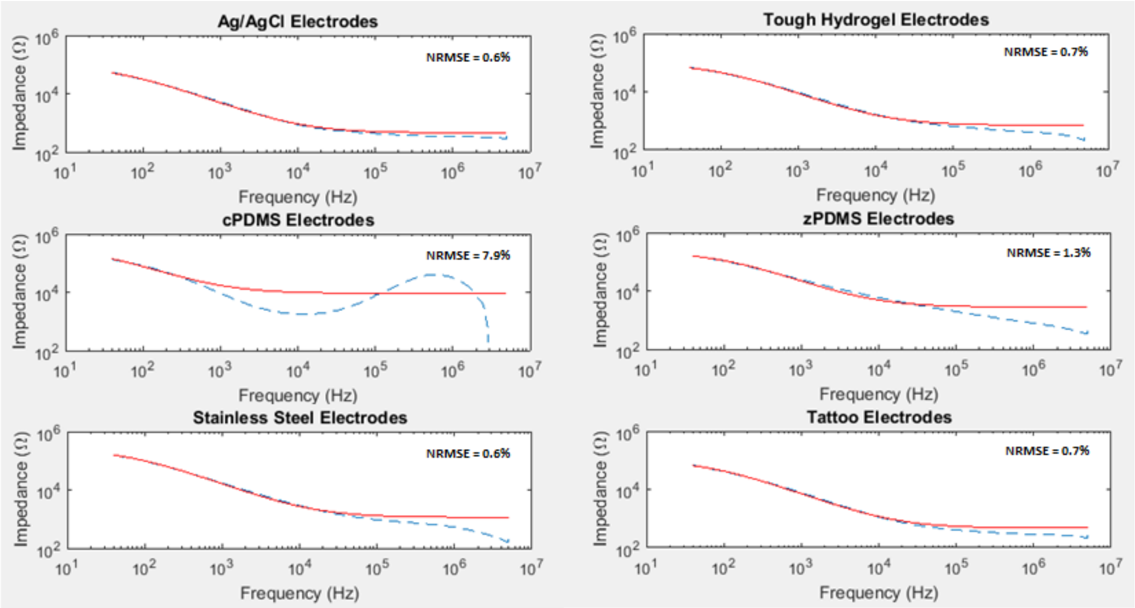

Figure 4.4: Experimental results (blue) and the fitting curve (red) for each electrode-skin impedance frequency response and the respective mean square error associated to the fitting curve.

The estimated values of the circuit model components for all tested electrodes are presented in table 4.1. As previously stated, the component R_d represents the resistance to the movement of the charges between the electrode and the skin. This way a high R_d value reflects in a high electrode-skin impedance, which results in a poor biological signal quality. Moreover, the C_d component represents the charges exchange between the electrode and skin and the R_s the resistance of the electrolyte or sweat. Therefore, for health devices, a low R_d, low R_s and high C_d values are desired in order to increase the biological signal quality [50].

Table 4.1: Circuit components values for all electrodes with approximately the same area and distance between them.

Electrode	**R_s (Ω)**	**R_d (kΩ)**	**C_d (nF)**
Ag/AgCl	454.3	90.6	34.0
Square hydrogel-PDMS	712.4	91.6	17.9
Stainless Steel	1153.5	257.7	9.9
zPDMS	2783.3	216.1	7.6
cPDMS	9164.9	356.8	19.3
Tattoo	472.3	101.9	22.4

The Ag/AgCl electrodes exhibit the lowest R_d and R_s values of all electrodes. Like these electrodes, hydrogel-PDMS electrodes have gel in their constitution which causes a decrease in the resistance to the ionic current of the body and provides a better attachment to the skin than other electrodes. This results in low values of R_d and R_s. This way, the R_d value for the hydrogel-PDMS electrode is similar to the Ag/AgCl electrode. When comparing to stainless steel, zPDMS and cPDMs, the R_s value of the hydrogel-PDMS electrodes are smaller. However, there is a slight difference between the hydrogel and the Ag/AgCl electrodes value. This difference can be justified since the measurements with the hydrogel electrodes were not made on the same day as the other electrodes. Therefore, the sweat secretion level could have been different, which influence the R_s value.

Low values of R_s were also obtained for the tattoo electrodes that are lower than the hydrogel-PDMS. The tattoo electrodes are probably the ones that have a better adhesion since the tattoo paper glues to the skin. However, they can only be used one time. Their R_s value is higher than the hydrogel-PDMS and Ag/AgCl electrodes.

The R_d and R_s values of zPDMS and cPDMS electrodes are must higher than the values of the others electrodes, which may indicate that the circuit model suggested do not explain the impedance of these electrodes. This is proven by the high error associated with the fitting curve.

The higher the C_d value, the better is the biological signal quality [50]. As for the other components value, the Ag/AgCl electrodes seems the best, since they present a higher value of C_d. The tattoo electrodes exhibit a higher C_d than the hydrogel-PDMS electrode but smaller than the Ag/AgCl. Even being smaller, the C_d value of hydrogel-PDMS electrode is not that distance from the tattoo electrode value. The small C_d value for the stainless steel electrode is due to the accumulation of charges on electrode-skin interface, since these are polarizable electrodes [50]

The Ag/AgCl electrodes are the most commonly used electrode for biopotential measurement. These electrodes exhibit the best combination of values for the circuit model components which result in a high biological signal quality. However, the Ag/AgCl electrodes are only intended to be use one time and are not stretchable. On the other hand, a hydrogel-PDMS conjunction originates stretchable and reusable electrodes, which have shown a low electrode-skin impedance.

The impedance for two different sets of hydrogel-PDMS electrodes was measured: square and round electrodes. Besides having different shapes, the round hydrogel-PDMS electrodes were made long before the square electrodes. Therefore, the number of utilizations at the moment of the impedance measurement was a lot superior to the square electrodes. The Bode plot obtained for each electrode and the respective fitting curve are presented in 4.5.

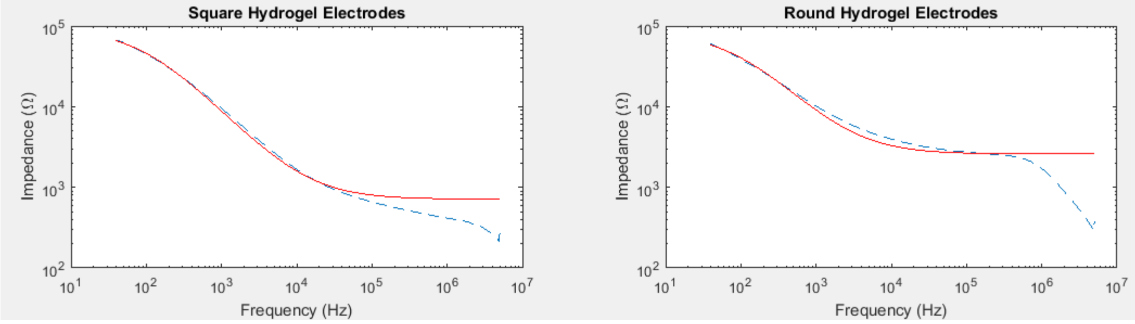

Figure 4.5: Experimental results (blue) and the fitting curve (red) for both hydrogel-PDMS electrode-skin impedance frequency response.

Through the analyse of the Bode plots, it is possible to observe a small increase on the impedance from the square to the round hydrogel-PDMS electrodes. As the hydrogel-PDMS electrodes have different shapes, the circuit components values for each are presented by square centimetre in table 4.2.

Table 4.2: Circuit components values for the two types of hydrogel-PDMS electrodes per square centimetre.

Hydrogel electrodes	**R$_s$ (Ω/cm^2)**	**R$_d$ (kΩ/cm^2)**	**C$_d$ (nF/cm^2)**
Square	508.9	65.4	12.8
Round	1192.7	37.1	10.4

Even though the R$_s$ value of the round hydrogel-PDMS electrodes is twice the value of the square, the value of R$_d$ is much smaller and the C$_d$ is not much different. The big difference on the R$_s$ values could be explained by the existence of different hydrogels' concentration induce by distinct evaporation rates. Even more, the distance between the electrodes was almost double in the round electrodes, which could induce changes in theses values. This suggests that over time and utilizations the circuit component values could not change much.

4.4 Soft EMG sensor and signal acquisition

The impedance analysis shows that hydrogel-PDMS electrodes exhibit low electrode-skin impedance and therefore, could be used for biopotential measurement. In order to prove this possibility, EMG sensors were developed and signals from two different muscles were obtained.

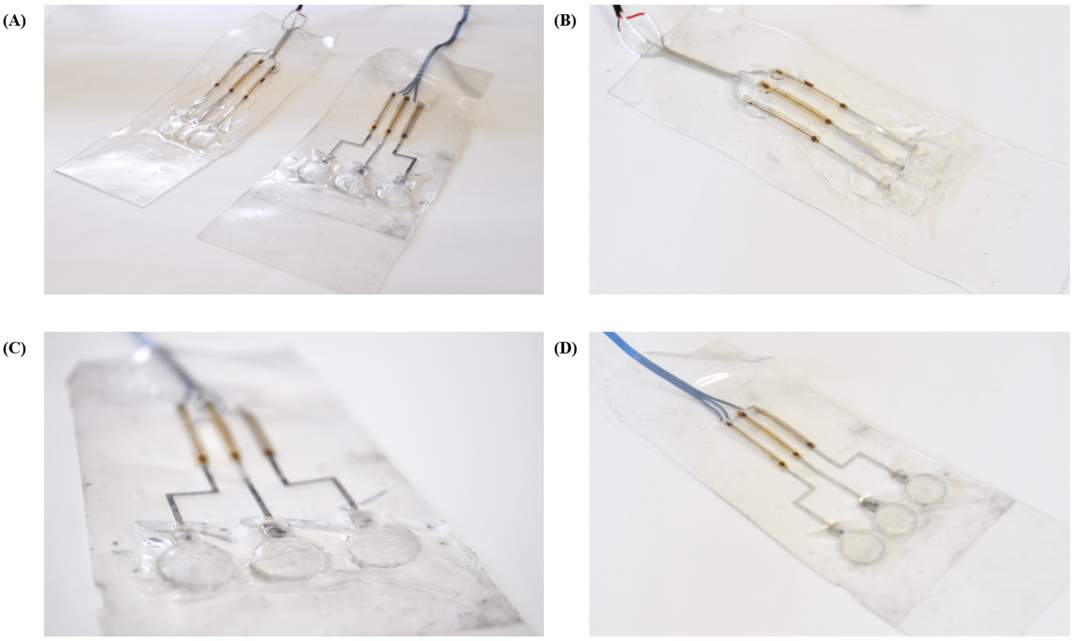

Figure 4.6: **(A)** Two soft EMG sensors were developed with hydrogel-PDMS electrodes. **(B)** Square hydrogel-electrodes were used to fabricate one of the EMG sensors and **(C), (D)** round electrodes for the other.

The EMG sensor with round hydrogel-PDMS electrodes (figure 4.6(**C**), (**D**)) was placed on the ventral side of the forearm in order to detect the flexor carpi radialis muscle as previously said. The sensor with square hydrogel-PDMS electrodes (figure 4.6(**B**)) was attached to the skin in the position of the flexor carpi ulnaris muscle. In order to validate the acquired signal, signals with stainless steel electrodes were also acquired on both of these muscles. The same three movements were performed with all sensors: fist clenching, wrist flexion and opening the hand.

The acquired signal from the round hydrogel and the stainless steel electrodes are present in the figures 4.7, 4.8 and 4.9. Through the analysis of the signals, it is possible to verify that the signals obtained with the hydrogel-PDMS electrodes are similar to the stainless steel electrodes. The flexion of the wrist originates a slightly higher amplitude on the signal with the proposed sensor than with the stainless steel electrodes. The others signals have approximately the same amplitude. Even more, the baseline for both sensors is nearly the same. However, there are more fluctuations on the hydrogel-PDMS electrodes baseline.

(A)

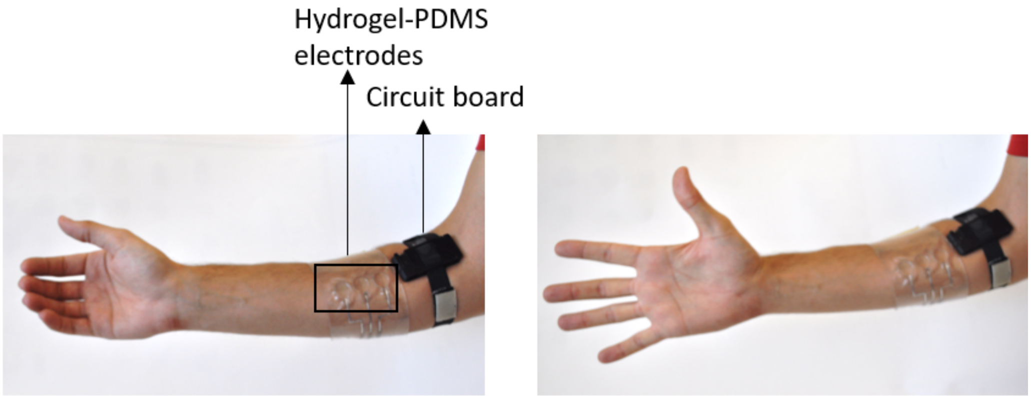
Hydrogel-PDMS electrodes
Circuit board

(B) Metal electrodes

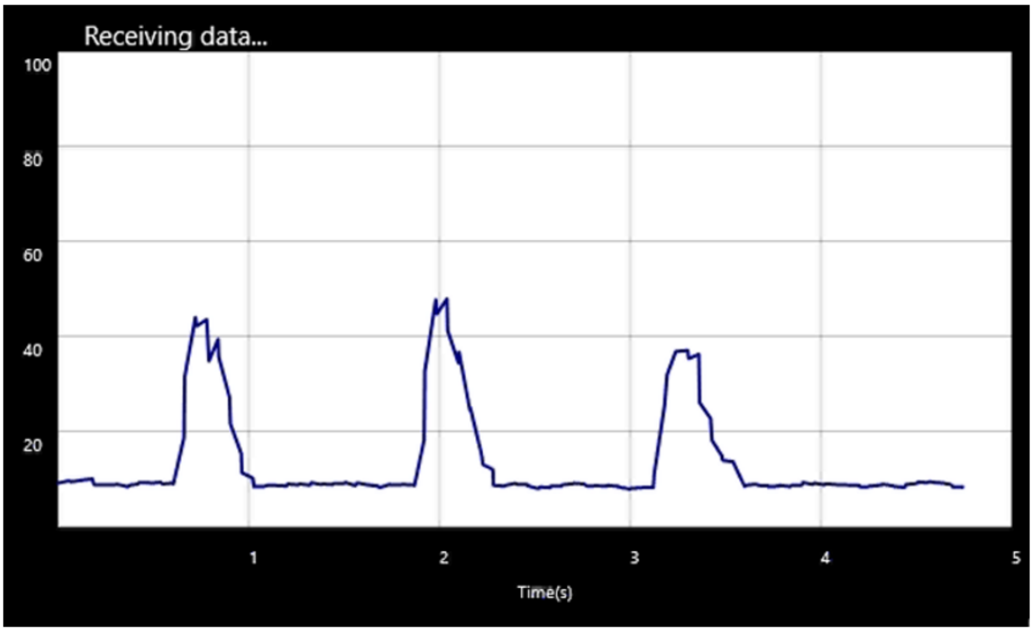

(C) Hydrogel-PDMS electrodes

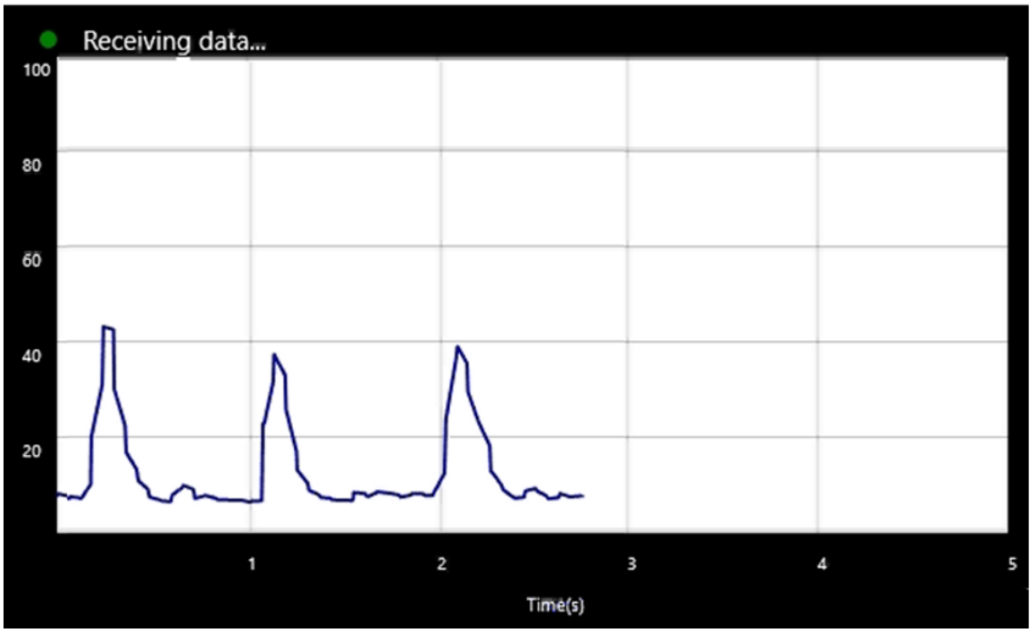

Figure 4.7: **(A)** Movement of opening the hand. **(B)** Signal with the stainless steel electrodes. **(C)** Signal with the round hydrogel-PDMS electrodes.

(A)

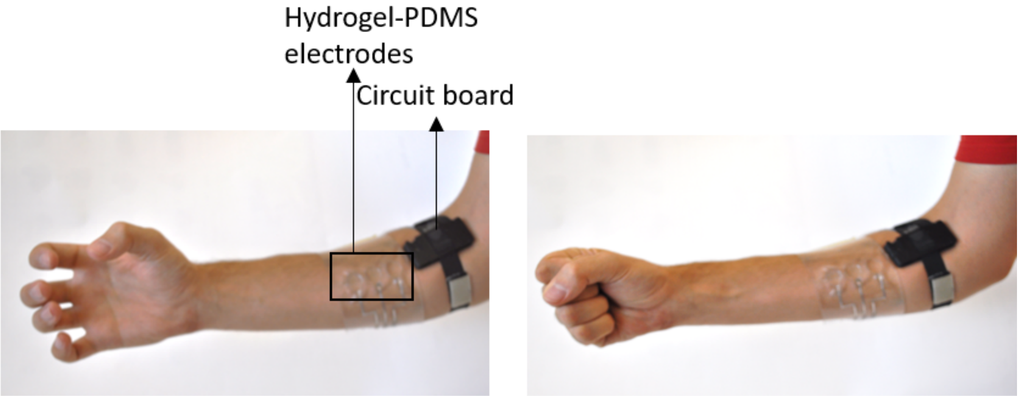
Hydrogel-PDMS electrodes
Circuit board

(B) Metal electrodes

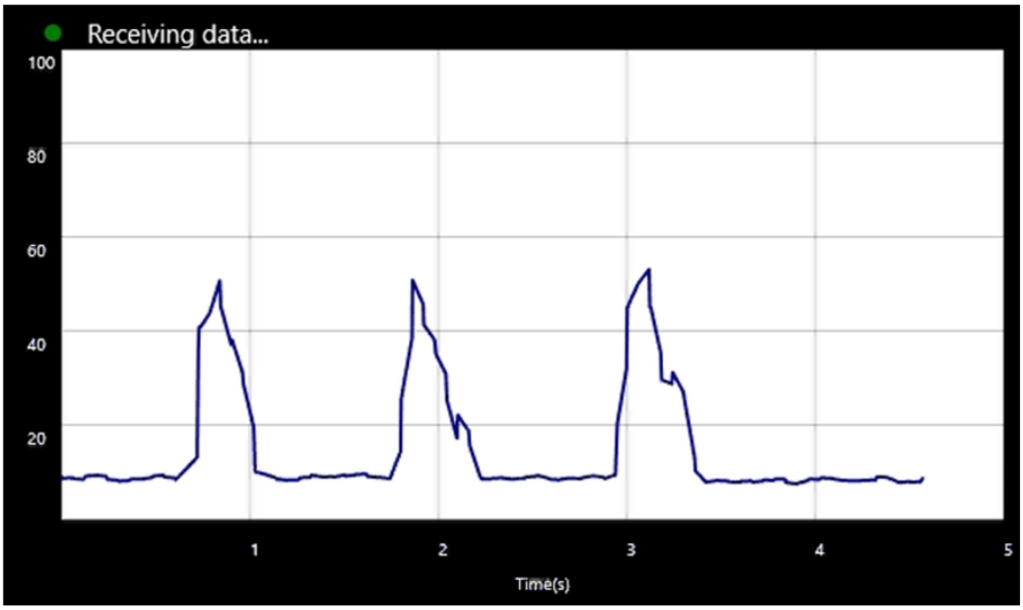

(C) Hydrogel-PDMS electrodes

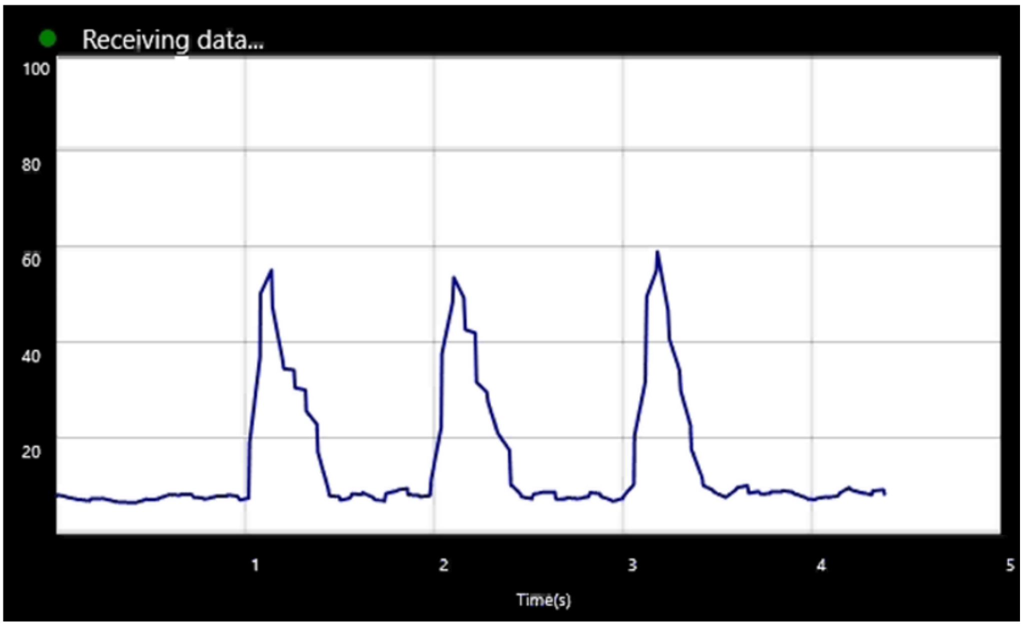

Figure 4.8: **(A)** Movement of fist clenching. **(B)** Signal with the stainless steel electrodes. **(C)** Signal with the hydrogel-PDMS electrodes.

(A)

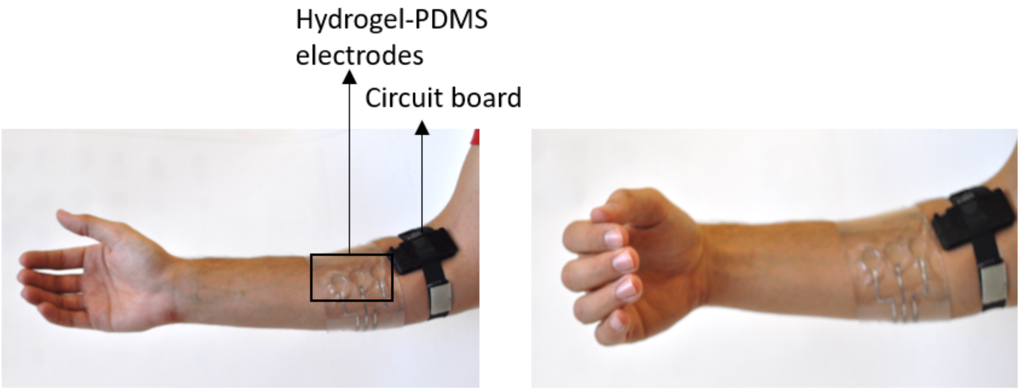
Hydrogel-PDMS electrodes
Circuit board

(B) Metal electrodes

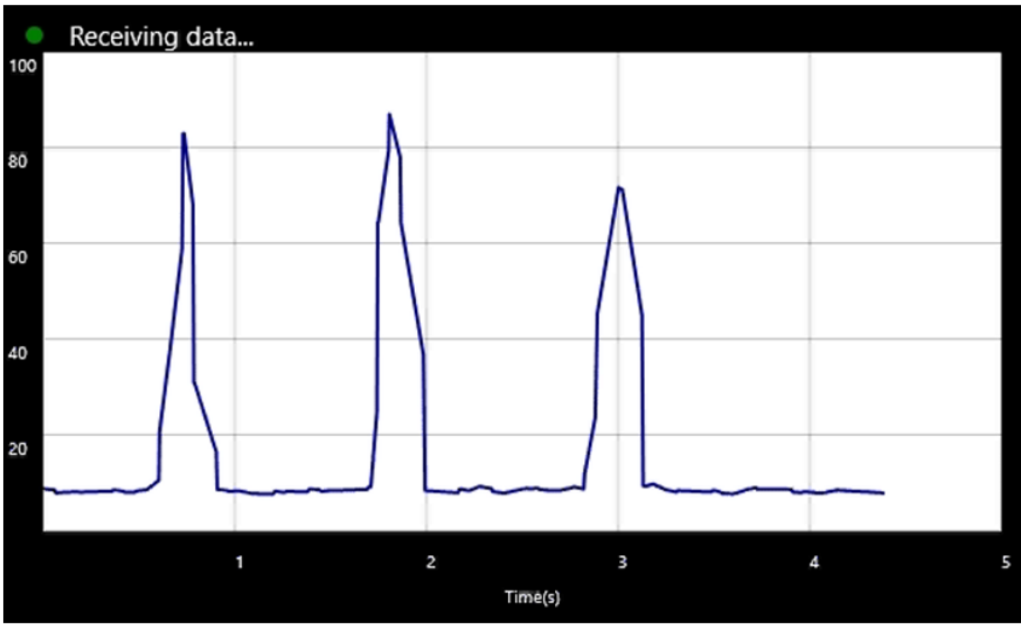

(C) Hydrogel-PDMS electrodes

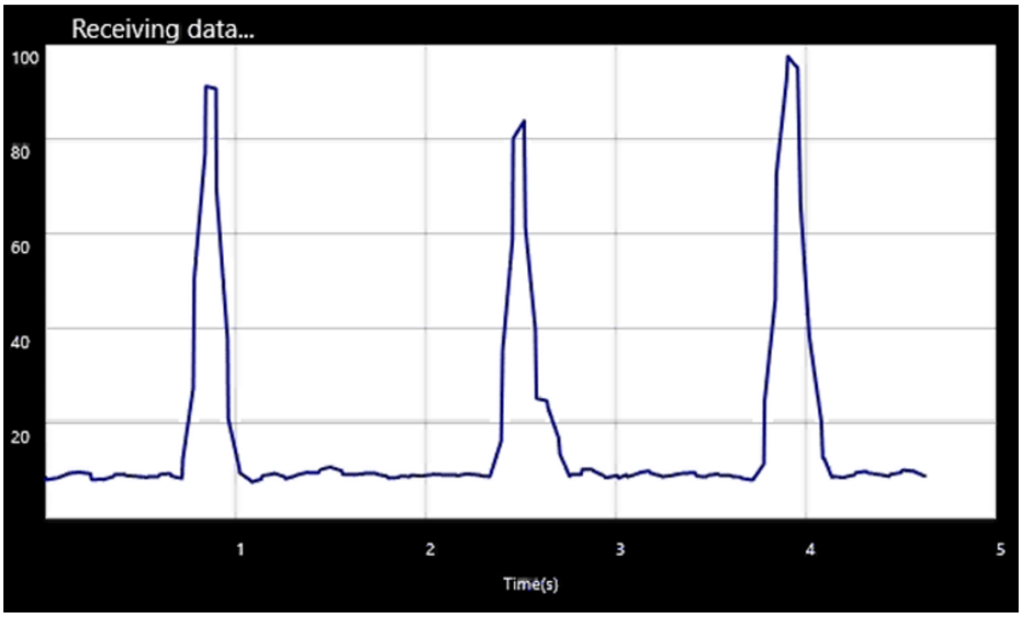

Figure 4.9: **(A)** Flexion of the wrist. **(B)** Signal with the stainless steel electrodes. **(C)** Signal with the hydrogel-PDMS electrodes.

The signal from the flexor carpi ulnaris muscle was also recorded with the square hydrogel-PDMS electrodes (figure 4.10). Like the signals of the other muscles, the signals from hydrogel-PDMS electrodes are really close to signal obtained with the stainless steel electrodes. Thus proving that hydrogel-PDMS conjunctions can be applied for detecting muscle activity through EMG. Even though when the water evaporated from the hydrogel, we could detect a small EMG signal and by submerging the electrodes on the sodium chloride solution with the initial concentration it returned to the normal signal.

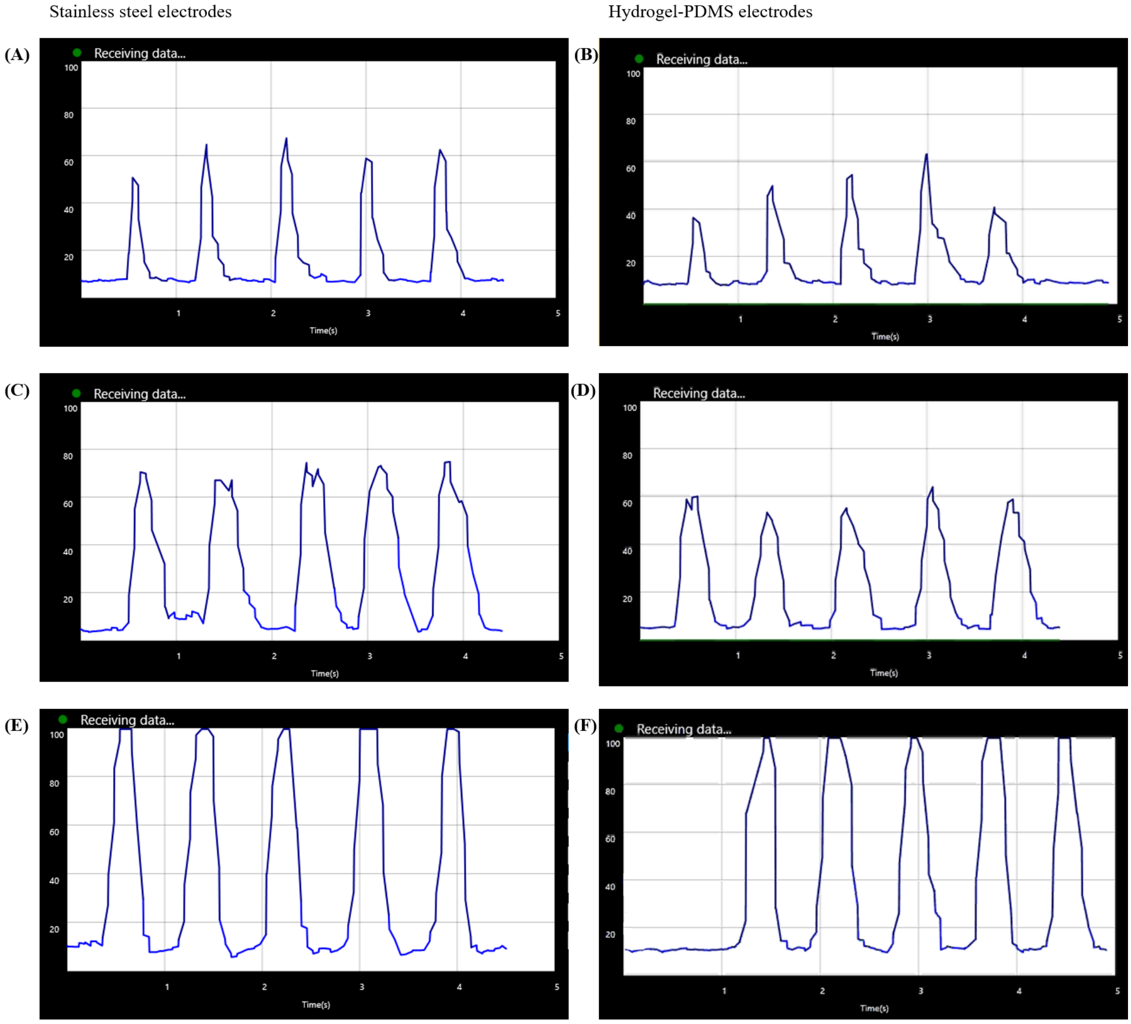
Stainless steel electrodes

Hydrogel-PDMS electrodes

Figure 4.10: Signals acquired with the **(A), (B)** opening of the hand, **(C),(D)** clenching the wrist and **(C),(D)** during wrist flexion.

4.5 GSR sensor and measurements

As previously said, skin resistance changes due to variation in sweat concentration. As hydrogel-PDMS electrodes present a low electrode-skin impedance and are mostly composed of water, in this work the possibility of applying them for GSR measurement was tested.

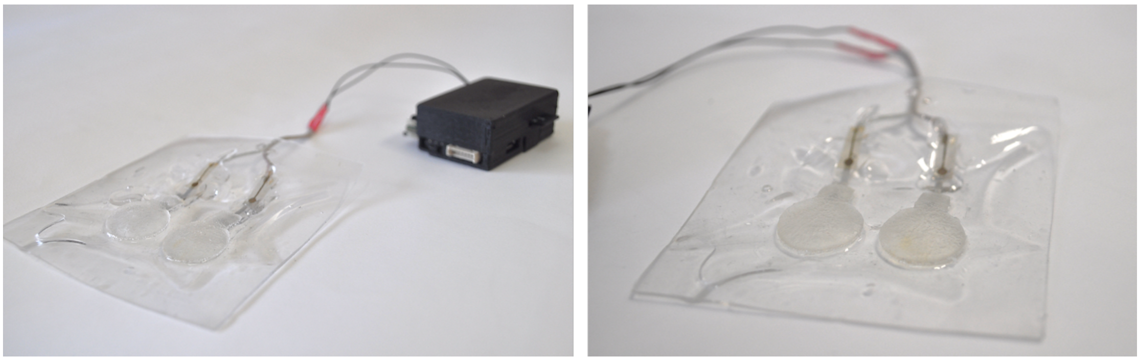

Figure 4.11: GSR sensor proposed in this work. The sensor consists in a multilayer system with hydrogel-PDMS electrodes, EGaIn and FPCBs as interconnects.

In the figure 4.12, plots from the static test using stainless steel electrodes and hydrogel-PDMS electrodes are presented. Through the analyse of these plots, it is evident the difference between both signal behaviour. The stainless steel electrodes take a longer time to achieve a steady state level than the hydrogel-PDMS electrodes, due to the inherent high contact stainless steel electrodes-skin resistance. Over time the sweat level located on the contact region built up leading to a decrease in the measured value. Concerning to hydrogel-PDMS electrodes, as they present low contact resistance due to the existence of an electrolyte solution in their composition, they are capable of detecting the real value of skin impedance right after placing in contact with the skin. The peaks on the hydrogel-PDMS electrodes signal (figure 4.12 **(B)**), it is possible to see some peaks due to movements or external stimuli since the subject was performing his daily routine at the laboratory.

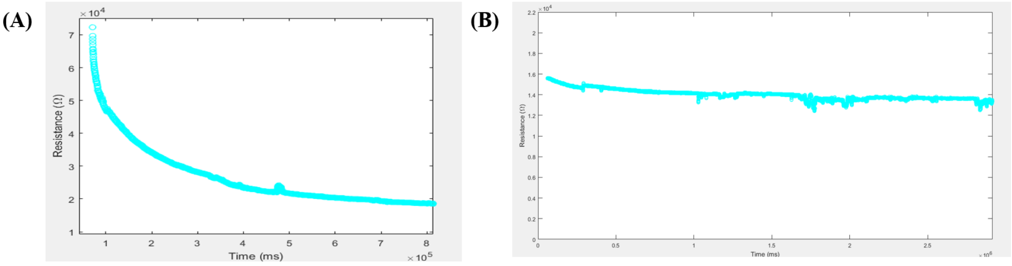

Figure 4.12: Skin resistance measures over time during daily activities for **(A)** Stainless steel electrodes and **(B)** the hydrogel-PDMS electrodes.

During physical activity the sweat secretion increases which consequently decrease the skin impedance. When the subject starts an intense activity, as cycling uphill, there is a significant decrease in the skin impedance. After the intense effort, the sweat secretion gradually stabilizes to the normal value, reaching approximately the initial value. The skin resistance signal during the physical activity test is present in figure 4.13. The signal was filtered with a low pass filter (with 900 points) was used to diminish the motion artifacts and other noise.

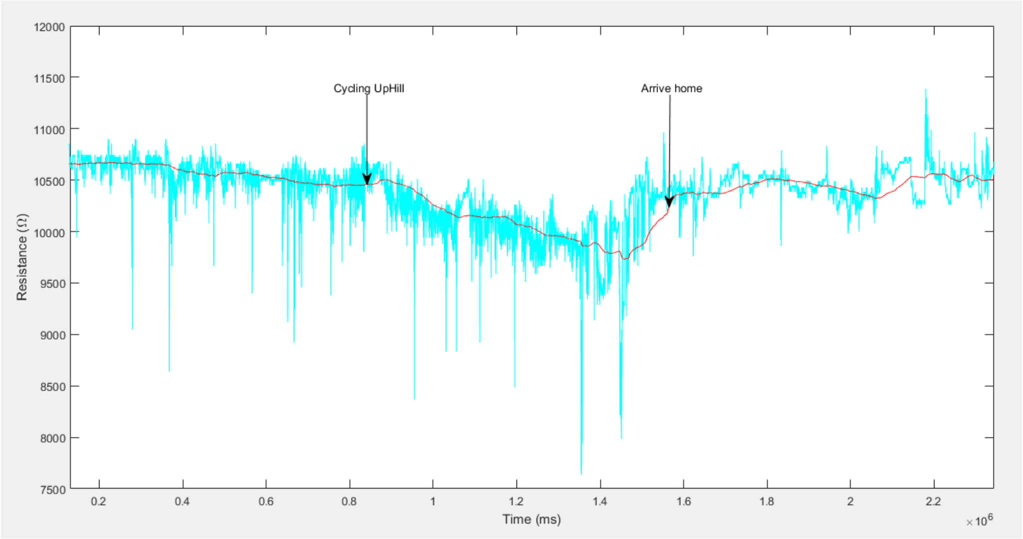

Figure 4.13: Skin resistance signal collected during physical exercise (blue) and the filtered signal (red).

As pointed out on the plot, when the subject starts the intense exercise as cycling uphill, the skin resistance begins decreasing. After achieving a maximum value of sweat secretion, the secretion stops and the sweat starts to evaporate, leading to and an increase in skin resistance. As expected, after arriving home the skin resistance goes back to the initial value.

Moreover, we tested the designed GSR sensor for stress detection by applying unexpected sonorous stimuli, while the subject was listening to meditation music (figure 4.14). A low pass filter (with 100 points) was applied to the signal in order to reduce the noise. From the beginning of the recording until shortly before of the first horror movie started, the subject was listening to meditation music. While not all changes are notable, we can see some decreases in the skin resistance. The more evident decline is at the beginning of the horror movie. As it is possible to verify the skin resistance was still decreasing when the stimuli were applied. This could be the reason why we were not able to detect all changes. Additionally, when the subject was tested he already had an idea of what was going to happen and thus did not have enough stimuli.

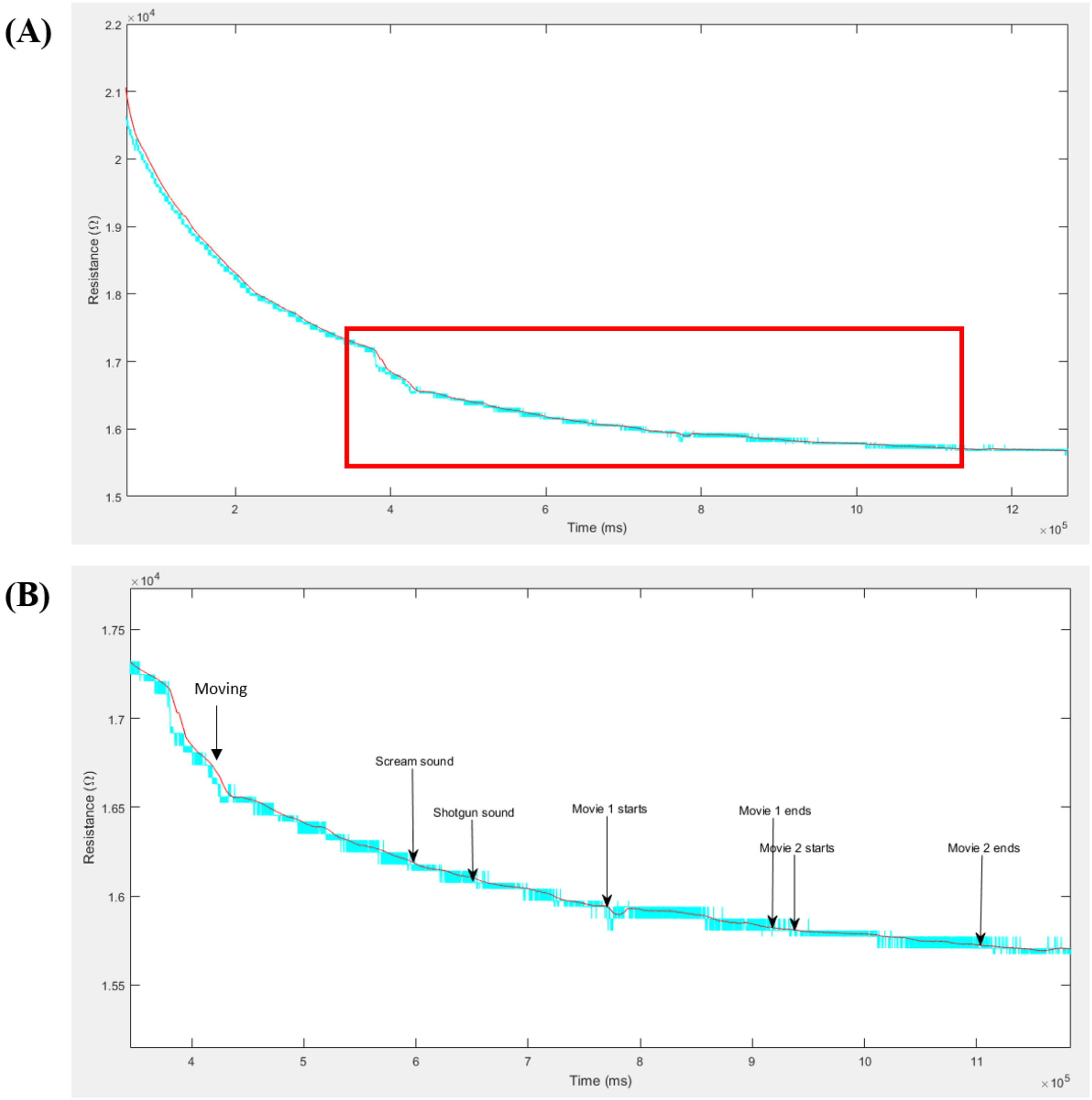

Figure 4.14: **(A)** Detected changes on skin resistance induced by sonorous stimuli (blue) and the filtered signal (red). **(B)** Zoom from area of interested.

These GSR case study is very preliminary and not conclusive. The tests were done as an initial step for future analysis which can include studying several subjects during a long period.

In addition, since the sweat composition can change the conductivity of hydrogel, it is not certain if a hydrogel electrode is also appropriate for GSR. Nevertheless, as previously stated the main advantage of hydrogel based electrodes is that they may allow sweat analysis which can be a subject for future studies.

4.6 Conclusion

In this chapter, two different case studies of biomonitoring systems based on hydrogel-PDMS electrodes were presented:

- EMG sensors
- GSR sensor

The soft EMG sensors with hydrogel-PDMS electrodes have proven that these electrodes are able of detecting biopotentials, similar to the stainless steel electrodes. On the other hand, the GSR sensor needs further tests since our results are not conclusive.

The impedance analysis showed that hydrogel-PDMS based electrodes exhibit low electrode-skin impedance, close to the Ag/AgCl and Tattoo electrodes. However, in contrast to theses last electrodes, hydrogel-PDMs hybrids are stretchable and can be reusable.

Furthermore, the dehydration test demonstrated that when in contact with the skin the water loss from the hydrogel is done gradually. This behaviour supports the use of hydrogel as a material for skin interface.

Chapter 5

Conclusions

In this work, a successful combination of PDMS based stretchable electronics with hydrogel electrodes was presented. This included obtaining the know-how for development of hydrogel-PDMS conjunctions, and then combine it with the existing know-how on stretchable electronics, in order to develop comprehensive biomonitoring patches that are able to make an excellent skin interface through hydrogels, and at the same time contain all necessary electrical circuit in the PDMS substrate.

The hydrogel-PDMS hybrid developed over this project shows great potential for biomonitoring applications. The high water content on the tough hydrogel, the high stretchability and permeability to different molecules make them attractive to use as skin interface. As proven by the dehydration test, when in contact with the skin the water loss is delayed, allowing the use of a sensor with this electrodes for a long time. Even so, if the water evaporates completely, by submerging the electrodes in an electrolyte solution it can return back to the initial performance.

Moreover, the impedance analysis confirmed that electrodes with hydrogel-PDMS hybrid show low electrode-skin impedance, which leads to a good signal quality. Other electrodes have shown low electrode-skin resistance, such as Ag/AgCl and tattoo electrodes. However, they do not exhibit stretchability and/or can only be used once. Therefore, hydrogel-PDMS electrodes can be a better choice since they can measure biopotential, present high quality of the biological signal, they are stretchable and can be reusable.

In addition, methods used for interfacing the conductive electrodes with liquid metal based interconnects on the PDMS were very reliable. The interface between conductive hydrogel and liquid metal was functional during several hours of testing.

With the aim to demonstrate the applicability of the hydrogel-PDMS electrodes, a GSR and EMG sensors were developed. In contrast to the metal electrodes, the hydrogel-PDMS electrodes adhere well to the epidermis and are stretchable. On the proposed GSR sensor, during physical activity, it was possible to detect the changes in the skin resistance. Preliminary GSR tests with hydrogel electrodes showed a better signal acquisition compared to dry steel electrodes, but more deep analysis is required to perform emotional computing with hydrogel based electrodes.

5.1 Future work

The present work is an important contribution for wearable health devices fabrication, as two different functional sensors with hydrogel-PDMS electrodes were successfully developed.

Since the impedance of hydrogel-PDMS electrodes with a high number of utilizations was not far from the impedance obtained for new electrodes, it may be interesting to study the reproducibility of sensors with these electrodes.

Furthermore, hydrogel-PDMS electrodes are able to detect changes in sweat secretion and they are permeable to this body fluid, they can be used for sweat analysis. Therefore, additional studies can be done in order to understand the incorporation of biomarkers into the hydrogel matrix for sweat analysis. Even more, studies involving the fabrication of microfluidic devices with this tough hydrogel-PDMS conjunction for collection and analysis of sweat can be very promising.

Additionally, further tests can be done with the GSR sensor with several subjects and different step up. The frequency used in this project could not be the best, therefore, the impedance response can be acquired for all frequencies. A possible future approach can be using the GSR sensor with hydrogel-PDMS electrodes for an emotion classifications algorithm.

Bibliography

[1] Wearable Technology 2017-2027: Markets, Players, Forecasts: IDTechEx. http://www.idtechex.com/research/reports/wearable-technology-2017-2027-markets-players-forecasts-000536.asp?viewopt=showall. (Acessed 4 August 2017).

[2] Wearable Sensors 2016-2026: Market Forecasts, Technologies, Players: IDTechEx. http://www.idtechex.com/research/reports/wearable-sensors-2016-2026-market-forecasts-technologies-players-000470.asp. (Acessed 4 August 2017).

[3] James J S Norton, Dong Sup Lee, Jung Woo Lee, Woosik Lee, Ohjin Kwon, Phillip Won, Sung-Young Jung, Huanyu Cheng, Jae-Woong Jeong, Abdullah Akce, Stephen Umunna, Ilyoun Na, Yong Ho Kwon, Xiao-Qi Wang, ZhuangJian Liu, Ungyu Paik, Yonggang Huang, Timothy Bretl, Woon-Hong Yeo, and John A Rogers. Soft, curved electrode systems capable of integration on the auricle as a persistent brain–computer interface. *Proceedings of the National Academy of Sciences*, 112(13):3920–3925, 2015.

[4] Dae-Hyeong Kim, Nanshu Lu, Rui Ma, Yun-Soung Kim, Rak-Hwan Kim, Shuodao Wang, Jian Wu, Sang Min Won, Hu Tao, Ahmad Islam, Ki Jun Yu, Tae-il Kim, Raeed Chowdhury, Ming Ying, Lizhi Xu, Ming Li, Hyun-Joong Chung, Hohyun Keum, Martin McCormick, Ping Liu, Yong-Wei Zhang, Fiorenzo G Omenetto, Yonggang Huang, Todd Coleman, and John A Rogers. Epidermal Electronics. *Science*, 333(6044):838–843, 2011.

[5] Y. Liu, James J S Norton, Raza Qazi, Zhanan Zou, Kaitlyn R Ammann, Hank Liu, Lingqing Yan, Phat L Tran, K.-I. Jang, Jung Woo Lee, Douglas Zhang, Kristopher A Kilian, Sung Hee Jung, Timothy Bretl, Jianliang Xiao, Marvin J Slepian, Yonggang Huang, J.-W. Jeong, and John A Rogers. Epidermal mechano-acoustic sensing electronics for cardiovascular diagnostics and human-machine interfaces. *Science Advances*, 2(11):e1601185–e1601185, 2016.

[6] Alessandra Zucca, Christian Cipriani, Sudha, Sergio Tarantino, Davide Ricci, Virgilio Mattoli, and Francesco Greco. Tattoo Conductive Polymer Nanosheets for Skin-Contact Applications. *Advanced Healthcare Materials*, 4(7):983–990, 2015.

[7] Namyun Kim, Taehoon Lim, Kwangsun Song, Sung Yang, and Jongho Lee. Stretchable Multichannel Electromyography Sensor Array Covering Large Area for Controlling Home Electronics with Distinguishable Signals from Multiple Muscles. *ACS Applied Materials and Interfaces*, 8(32):21070–21076, 2016.

[8] Michael D. Bartlett, Eric J. Markvicka, and Carmel Majidi. Rapid Fabrication of Soft, Multilayered Electronics for Wearable Biomonitoring. *Advanced Functional Materials*, 26(46):8496–8504, 2016.

[9] Ying Chen, Bingwei Lu, Yihao Chen, and Xue Feng. Breathable and Stretchable Temperature Sensors Inspired by Skin. *Scientific reports*, 5:11505, 2015.

[10] Ft Sun, Cynthia Kuo, Ht Cheng, S Buthpitiya, Patricia Collins, and Martin Griss. Activity-aware Mental Stress Detection Using Physiological Sensors. *Mobile Computing, Applications, and Services*, 76:1–20, 2012.

[11] Ming-Zher Poh, Nicholas C. Swenson, and Rosalind W. Picard. A wearable sensor for unobtrusive, long-term assesment of electrodermal activity. *IEEE Transactions on Biomedical Engineering*, 57(5):1243–1252, 2010.

[12] Jeehoon Kim, Sungjun Kwon, Sangwon Seo, and Kwangsuk Park. Highly wearable galvanic skin response sensor using flexible and conductive polymer foam. *Confer-*

ence proceedings : ... Annual International Conference of the IEEE Engineering in Medicine and Biology Society. IEEE Engineering in Medicine and Biology Society. Annual Conference, 2014(Figure 1):6631–6634, 2014.

[13] Mahmoud Tavakoli, Carlo Benussi, and Joao Luis Lourenco. Single channel surface EMG control of advanced prosthetic hands: A simple, low cost and efficient approach. *Expert Systems with Applications*, 79:322–332, 2017.

[14] Martin Weigel, Tong Lu, Gilles Bailly, Antti Oulasvirta, Carmel Majidi, and Jürgen Steimle. iSkin: Flexible, Stretchable and Visually Customizable On-Body Touch Sensors for Mobile Computing. *Proceedings of the 33rd Annual ACM Conference on Human Factors in Computing Systems - CHI '15*, pages 2991–3000, 2015.

[15] Thalmic Labs — Makers of the Myo Gesture Control Armband. https://www.thalmic.com/. (Acessed 26 August 2017).

[16] Kyung-In Jang, Sang Youn Han, Sheng Xu, Kyle E Mathewson, Yihui Zhang, Jae-Woong Jeong, Gwang-Tae Kim, R Chad Webb, Jung Woo Lee, Thomas J Dawidczyk, Rak Hwan Kim, Young Min Song, Woon-Hong Yeo, Stanley Kim, Huanyu Cheng, Sang Il Rhee, Jeahoon Chung, Byunggik Kim, Ha Uk Chung, Dongjun Lee, Yiyuan Yang, Moongee Cho, John G Gaspar, Ronald Carbonari, Monica Fabiani, Gabriele Gratton, Yonggang Huang, and John A Rogers. Rugged and breathable forms of stretchable electronics with adherent composite substrates for transcutaneous monitoring. *Nature communications*, 5:4779, 2014.

[17] Jungil Choi, Daeshik Kang, Seungyong Han, Sung Bong Kim, and John A. Rogers. Thin, Soft, Skin-Mounted Microfluidic Networks with Capillary Bursting Valves for Chrono-Sampling of Sweat. *Advanced Healthcare Materials*, 6(5):1601355, 2017.

[18] Ahyeon Koh, Daeshik Kang, Yeguang Xue, Seungmin Lee, Rafal M Pielak, Jeonghyun Kim, Taehwan Hwang, Seunghwan Min, Anthony Banks, Philippe Bastien, Megan C Manco, Liang Wang, Kaitlyn R Ammann, K.-I. Jang, Phillip Won, Seungyong Han, Roozbeh Ghaffari, Ungyu Paik, Marvin J Slepian, Guive Balooch,

Yonggang Huang, and John A Rogers. A soft, wearable microfluidic device for the capture, storage, and colorimetric sensing of sweat. *Science Translational Medicine*, 8(366):366ra165, 2016.

[19] Hyunwoo Yuk, Teng Zhang, German Alberto Parada, Xinyue Liu, and Xuanhe Zhao. Skin-inspired hydrogel-elastomer hybrid with robust interfaces and functional microstructures. *Nature Communications*, 7(May):1–11, 2016.

[20] Chao Chen, Zhengjin Wang, and Zhigang Suo. Flaw sensitivity of highly stretchable materials. *Extreme Mechanics Letters*, 10:50–57, 2017.

[21] T Maleki, G Chitnis, and B Ziaie. A batch-fabricated laser-micromachined PDMS actuator with stamped carbon grease electrodes. *Journal of Micromechanics and Microengineering*, 21(2):027002, 2011.

[22] Bo Wang, Bong Kee Lee, Min Joo Kwak, and Dong Weon Lee. Graphene/polydimethylsiloxane nanocomposite strain sensor. *Review of Scientific Instruments*, 84(10):105005, 2013.

[23] Yingying Zhang, Chris J. Sheehan, Junyi Zhai, Guifu Zou, Hongmei Luo, Jie Xiong, Y. T. Zhu, and Q. X. Jia. Polymer-embedded carbon nanotube ribbons for stretchable conductors. *Advanced Materials*, 22(28):3027–3031, 2010.

[24] Takeo Yamada, Yuhei Hayamizu, Yuki Yamamoto, Yoshiki Yomogida, Ali Izadi-Najafabadi, Don N Futaba, and Kenji Hata. A stretchable carbon nanotube strain sensor for human-motion detection. *Nature Nanotechnology*, 6(5):296–301, 2011.

[25] Feng Xu and Yong Zhu. Highly conductive and stretchable silver nanowire conductors. *Advanced Materials*, 24(37):5117–5122, 2012.

[26] Tahmina Akter and Woo Soo Kim. Reversibly Stretchable Transparent Conductive Coatings of Spray- Deposited Silver Nanowires(supporting). *ACS Applied Materials & Interfaces*, 4(4):1855–1859, 2012.

[27] Weili Hu, Ranran Wang, Yunfeng Lu, and Qibing Pei. An elastomeric transparent composite electrode based on copper nanowires and polyurethane. *Journal of Materials Chemistry C*, 2(7):1298, 2014.

[28] Michael D. Dickey. Emerging applications of liquid metals featuring surface oxides. *ACS Applied Materials and Interfaces*, 6(21):18369–18379, 2014.

[29] Mahmoud Tavakoli, Rui Rocha, Luis Osorio, Miguel Almeida, Anibal de Almeida, Vivek Ramachandran, Arya Tabatabai, Tong Lu, and Carmel Majidi. Carbon doped PDMS: conductance stability over time and implications for additive manufacturing of stretchable electronics. *Journal of Micromechanics and Microengineering*, 27(3):035010, 2017.

[30] Sang-Min Park, Nam-Su Jang, Sung-Hun Ha, Kang Hyun Kim, Dong-Wook Jeong, Jeonghyo Kim, Jaebeom Lee, S. H. Kim, and Jong-Man Kim. Metal Nanowire Percolation Micro-Grids Embedded in Elastomer for Stretchable and Transparent Conductors. *J. Mater. Chem. C*, 3:8241–8247, 2015.

[31] Shakti Dwivedi, Pankaj Khatri, Gilhotra Ritu Mehra, and Vikash Kumar. Hydrogel-A Conceptual Overview. *IJPBA*, 2(6):1588–1597, 2011.

[32] Kosmas Deligkaris, Tadele Shiferaw Tadele, Wouter Olthuis, and Albert Van Den Berg. Hydrogel-based devices for biomedical applications. *Sensors & Actuators: B. Chemical*, 147(2):765–774, 2010.

[33] Hyunwoo Yuk, Teng Zhang, Shaoting Lin, German Alberto Parada, and Xuanhe Zhao. Tough Bonding of Hydrogels to Diverse Nonporous Surfaces. *Nature Materials*, 15:190–196, 2016.

[34] Can Hui, Baohong Chen, Jing Jing, Jian Hai, Jinxiong Zhou, Yong Mei, and Zhigang Suo. Ionic cable. *Extreme Mechanics Letters*, 3:59–65, 2015.

[35] Shaoting Lin, Hyunwoo Yuk, Teng Zhang, German Alberto Parada, and Hyunwoo Koo. Stretchable Hydrogel Electronics and Devices. *Advanced Materials*, 28:4497–

4505, 2016.

[36] Christoph Keplinger, Jeong-yun Sun, Choon Chiang Foo, Philipp Rothemund, George M Whitesides, and Zhigang Suo. Stretchable, Transparent, Ionic Conductors. *Science*, 341(6149):984–987, 2013.

[37] Jeong-yun Sun, Christoph Keplinger, George M Whitesides, and Zhigang Suo. Ionic Skin. *Advanced Materials*, pages 1–7, 2014.

[38] Chong-chan Kim, Hyun-hee Lee, Kyu Hwan Oh, and Jeong-yun Sun. Highly stretchable, transparent ionic touch panel. *Science*, 353(6300):2957–2961, 2016.

[39] Xinyue Liu, Tzu-Chieh Tang, Eléonore Tham, Hyunwoo Yuk, Shaoting Lin, Timothy K. Lu, and Xuanhe Zhao. Stretchable living materials and devices with hydrogel–elastomer hybrids hosting programmed cells. *Proceedings of the National Academy of Sciences*, 114(9):2200–2205, 2017.

[40] Qinyuan Chai, Yang Jiao, and Xinjun Yu. Hydrogels for Biomedical Applications : Their Characteristics and the Mechanisms behind Them. *Gels*, 3(1):6, 2017.

[41] Jeong-yun Sun, Xuanhe Zhao, Widusha R.K Illeperuma, Ovijit Chaudhuri, Kyu Hwan Oh, David J. Mooney, Joost J. Vlassak, and Zhigang Suo. Highly stretchable and tough hydrogels. *Nature*, 489(7414):133–136, 2012.

[42] Alvaro Mata, Aaron J. Fleischman, and Shuvo Roy. Characterization of polydimethylsiloxane (PDMS) properties for piomedical micro/nanosystems. *Biomedical Microdevices*, 7(4):281–293, 2005.

[43] Teruo Fujii. PDMS-based microfluidic devices for biomedical applications. *Microelectronic Engineering*, 61-62:907–914, 2002.

[44] Ieong Wong and Chih Ming Ho. Surface molecular property modifications for poly(dimethylsiloxane) (PDMS) based microfluidic devices. *Microfluidics and Nanofluidics*, 7(3):291–306, 2009.

[45] Marc H. Schneider, Yvette Tran, and Patrick Tabeling. Benzophenone absorption and diffusion in poly(dimethylsiloxane) and its role in graft photo-polymerization for surface modification. *Langmuir*, 27(3):1232–1240, 2011.

[46] Michael D. Dickey. Stretchable and Soft Electronics using Liquid Metals. *Advanced Materials*, 1606425:1–19, 2017.

[47] Hyung Jun Koo, Ju Hee So, Michael D. Dickey, and Orlin D. Velev. Towards all-soft matter circuits: Prototypes of quasi-liquid devices with memristor characteristics. *Advanced Materials*, 23(31):3559–3564, 2011.

[48] Ju Hee So, Hyung Jun Koo, Michael D. Dickey, and Orlin D. Velev. Ionic current rectification in soft-matter diodes with liquid-metal electrodes. *Advanced Functional Materials*, 22(3):625–631, 2012.

[49] A. I. Ancharov, T. F. Grigoryeva, A. P. Barinova, and V. V. Boldyrev. Interaction between copper and gallium. *Russian Metallurgy (Metally)*, 2008(6):475–479, 2009.

[50] Anas Albulbul. Evaluating Major Electrode Types for Idle Biological Signal Measurements for Modern Medical Technology. *Bioengineering*, 3(3):20, 2016.

[51] Department of Radiology, University of Washington - Flexor Carpi Ulnaris. https://rad.washington.edu/muscle-atlas/flexor-carpi-ulnaris/. (Acessed 4 September 2017).

[52] James E. Mark. *Polymer Data Handbook. Oxford University Press*. 1998.

Appendices

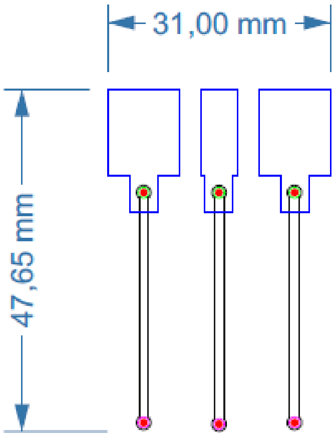
31,00 mm
47,65 mm

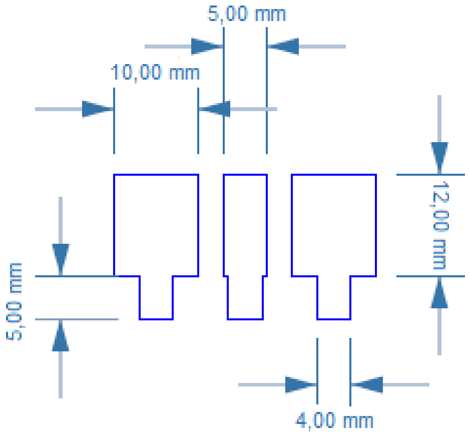
5,00 mm
10,00 mm
12,00 mm
5,00 mm
4,00 mm

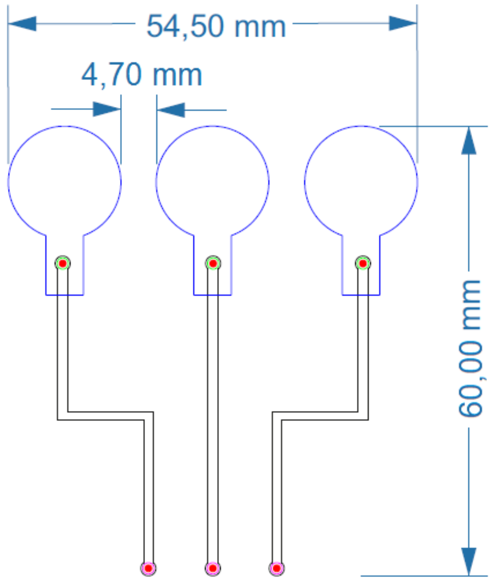
54,50 mm
4,70 mm
60,00 mm

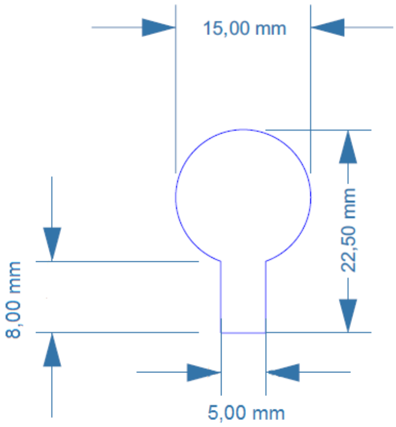
15,00 mm
22,50 mm
8,00 mm
5,00 mm

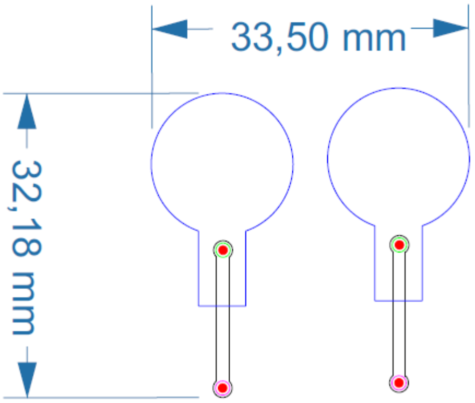
33,50 mm
32,18 mm

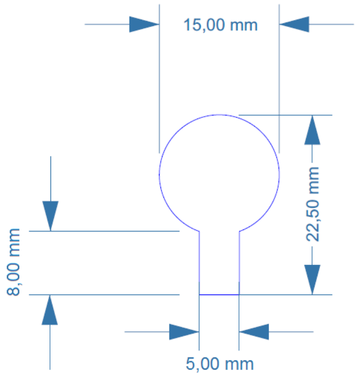
15,00 mm
22,50 mm
8,00 mm
5,00 mm

CONSENTIMENTO INFORMADO, ESCLARECIDO E LIVRE PARA PARTICIPAÇÃO EM ESTUDOS DE INVESTIGAÇÃO

Título do estudo: Medida da resistência da pele

Enquadramento: Teste efetuado no decorrer da dissertação de mestrado, intitulada *Hydrogel-PDMS conjunctions for stretchable electronics.* Dissertação desenvolvida na Faculdade de Ciências e Tecnologia da Universidade de Coimbra e supervisionada pelo Professor Doutor Mahmoud Tavakoli e pelo Professor Doutor Jorge Coelho.

Explicação do estudo: No decorrer deste estudo será recolhido o valor da resistência da pele durante três situações diferentes. A primeira situação consiste na medição da resistência da pele durante atividades quotidianas. A segunda, durante a realização de exercício físico, especificamente andar de bicicleta. Na terceira e última situação, a medição será feita durante um período de relaxamento, no qual serão aplicados alguns estímulos sonoros inesperados e serão mostrados dois excertos de um filme de terror.

A recolha dos dados será realizada no Instituto de Sistemas e Robótica da Universidade de Coimbra e implicará quatro medições.

Condições: A participação no estudo é inteiramente voluntária e a sua realização não implica qualquer risco para a integridade física ou saúde do participante.

Confidencialidade e anonimato: Os dados recolhidos serão exclusivamente utilizados no contexto da dissertação de mestrado acima referido e não será registado dados de identificação do participante.

Investigadora - Tatiana Alexandra Fernandes Patrício. Estudante do Mestrado Integrado em Engenharia Biomédica, na Universidade de Coimbra. Endereço eletrónico: tafp.14@gmail.com.

Por favor, leia com atenção a seguinte informação. Se achar que algo está incorreto ou que não está claro, não hesite em solicitar mais informações. Se concorda com a proposta que lhe foi feita, queira assinar este documento.

Assinatura de quem pede consentimento:

Tatiana Alexandra Fernandes Patrício

Declaro ter lido e compreendido este documento, bem como as informações verbais que me foram fornecidas pela pessoa que acima assina. Foi-me garantida a possibilidade de, em qualquer altura, recusar participar neste estudo sem qualquer tipo de consequências. Desta forma, aceito participar neste estudo e permito a utilização dos dados que de forma voluntária forneço, confiando em que apenas serão utilizados para esta investigação e nas garantias de confidencialidade e anonimato que me são dadas pela investigadora.

Nome: … João Daniel Green da Costa Ferreira Marques … … …

Assinatura: … … … Daniel Green … … … … … … … … … … … … **Data:** …1… / …09/ …2017…